Cancer Cell

Article

Putting the STING back into BH3-mimetic drugs for *TP53*-mutant blood cancers

Graphical abstract

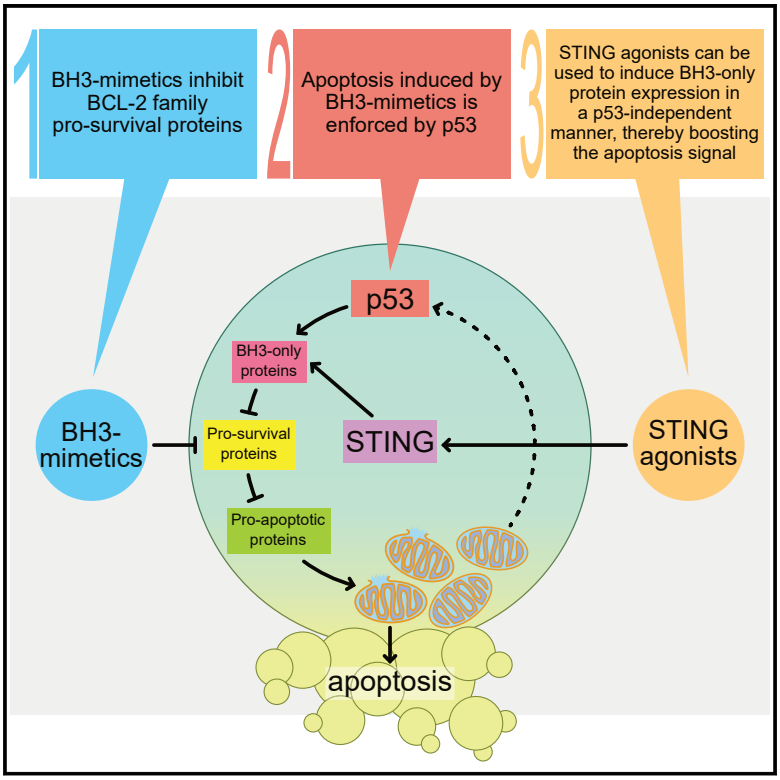

Highlights

- BH3-mimetic-induced MOMP activates p53 to enforce apoptosis in blood cancers
- STING pathway activation triggers p53-independent apoptosis in blood cancers
- STING agonists synergize with BH3-mimetics to kill *TP53*-mutant blood cancers

Authors

Sarah T. Diepstraten, Yin Yuan, John E. La Marca, ..., Andreas Strasser, Andrew H. Wei, Gemma L. Kelly

Correspondence

diepstraten.s@wehi.edu.au (S.T.D.), gkelly@wehi.edu.au (G.L.K.)

In brief

Diepstraten et al. demonstrate that p53 enforces apoptosis induced by BH3-mimetic drugs. To boost BH3-mimetic-induced apoptosis in *TP53*-mutant blood cancers, STING agonists were employed to induce pro-apoptotic BH3-only protein expression in a p53-independent manner. Therefore, BH3-mimetics alongside STING agonists represents a promising new combination therapy for aggressive *TP53*-mutant blood cancers.

Diepstraten et al., 2024, Cancer Cell *42*, 1–19
May 13, 2024
https://doi.org/10.1016/j.ccell.2024.04.004

CellPress

Please cite this article in press as: Diepstraten et al., Putting the STING back into BH3-mimetic drugs for *TP53*-mutant blood cancers, Cancer Cell (2024), https://doi.org/10.1016/j.ccell.2024.04.004

Cancer Cell

CellPress
OPEN ACCESS

Article

Putting the STING back into BH3-mimetic drugs for *TP53*-mutant blood cancers

Sarah T. Diepstraten,[1,2,8,*] Yin Yuan,[1,2,3,8] John E. La Marca,[1,2,4,5,8] Savannah Young,[1] Catherine Chang,[1] Lauren Whelan,[1] Aisling M. Ross,[1,7] Karla C. Fischer,[1,2] Giovanna Pomilio,[1] Rhiannon Morris,[1,2] Angela Georgiou,[1] Veronique Litalien,[1] Fiona C. Brown,[1,2,6] Andrew W. Roberts,[1,2,3] Andreas Strasser,[1,2,9] Andrew H. Wei,[1,2,3,9] and Gemma L. Kelly[1,2,9,10,*]

[1]Blood Cells and Blood Cancer Division, The Walter and Eliza Hall Institute of Medical Research, Parkville, VIC 3052, Australia
[2]Department of Medical Biology, University of Melbourne, Parkville, VIC 3052, Australia
[3]Department of Clinical Haematology, Peter MacCallum Cancer Centre and Royal Melbourne Hospital, Melbourne, VIC 3050, Australia
[4]Genome Engineering and Cancer Modelling Program, Olivia Newton-John Cancer Research Institute, Heidelberg, VIC 3084, Australia
[5]School of Cancer Medicine, La Trobe University, Melbourne, VIC 3086, Australia
[6]Australian Centre for Blood Diseases, Monash University, Melbourne, VIC 3004, Australia
[7]School of Medicine, Bernal Institute, Limerick Digital Cancer Research Centre & Health Research Institute, University of Limerick, Limerick, Ireland
[8]These authors contributed equally
[9]Senior authors
[10]Lead contact
*Correspondence: diepstraten.s@wehi.edu.au (S.T.D.), gkelly@wehi.edu.au (G.L.K.)
https://doi.org/10.1016/j.ccell.2024.04.004

SUMMARY

TP53-mutant blood cancers remain a clinical challenge. BH3-mimetic drugs inhibit BCL-2 pro-survival proteins, inducing cancer cell apoptosis. Despite acting downstream of p53, functional p53 is required for maximal cancer cell killing by BH3-mimetics through an unknown mechanism. Here, we report p53 is activated following BH3-mimetic induced mitochondrial outer membrane permeabilization, leading to BH3-only protein induction and thereby potentiating the pro-apoptotic signal. *TP53*-deficient lymphomas lack this feedforward loop, providing opportunities for survival and disease relapse after BH3-mimetic treatment. The therapeutic barrier imposed by defects in *TP53* can be overcome by direct activation of the cGAS/STING pathway, which promotes apoptosis of blood cancer cells through p53-independent BH3-only protein upregulation. Combining clinically relevant STING agonists with BH3-mimetic drugs efficiently kills *TRP53*/*TP53*-mutant mouse B lymphoma, human NK/T lymphoma, and acute myeloid leukemia cells. This represents a promising therapy regime that can be fast-tracked to tackle *TP53*-mutant blood cancers in the clinic.

INTRODUCTION

Overall blood cancer survival rates have improved over the last decade due to advancements in molecular profiling and novel therapeutic approaches.[1,2] However, *TP53* (murine: *Trp53*)-defective lymphoma and leukemia remains a major clinical challenge, with patients bearing such mutations considered adverse risk and associated with inferior survival outcomes.[3–6] *TP53*-mutant blood cancers are more resistant to cytotoxic drugs which induce cancer cell death via DNA damage, and also harbor defects in metabolism, genome stability and autophagy, which confer reduced sensitivity to diverse anti-cancer agents.[7] *TP53* mutations occur in up to 25% of acute myeloid leukemias (AMLs),[5,8] 25% of non-Hodgkin lymphomas (NHLs),[3] and up to 60% of natural killer/T (NKT) cell lymphomas.[9] Effective treatment approaches for *TP53*-mutated blood cancers are urgently needed.

In response to stresses including oncogene activation, DNA damaging cytotoxic drugs, or γ-radiation, p53 is activated and upregulates expression of pro-apoptotic BH3-only proteins (e.g., NOXA, PUMA, and BIM).[10] This intrinsic apoptotic signaling pathway is governed by the balance between pro-apoptotic and pro-survival members of the BCL-2 family.[11] Pro-apoptotic BH3-only proteins physically sequester pro-survival proteins (e.g., MCL-1, BCL-2, and BCL-XL), promoting pro-apoptotic effector (BAK/BAX) activation. Activated BAK/BAX causes mitochondrial outer membrane permeabilization (MOMP), which releases apoptogenic factors and triggers the caspase cascade for cell demolition. Of note, while MOMP has been called the "point of no return" for apoptotic cells, recent studies have demonstrated "limited/minority" MOMP—where some mitochondria remain intact—thereby providing cells with an escape mechanism from death.[12–14]

BH3-mimetic drugs are small molecule inhibitors which directly bind and inhibit pro-survival members of the BCL-2 family. Their development was seen as a major milestone toward a p53-agnostic therapeutic, as their use would allow for apoptosis induction downstream of p53. The BCL-2 selective BH3-mimetic venetoclax/ABT-199 is approved by regulatory authorities

Please cite this article in press as: Diepstraten et al., Putting the STING back into BH3-mimetic drugs for *TP53*-mutant blood cancers, Cancer Cell (2024), https://doi.org/10.1016/j.ccell.2024.04.004

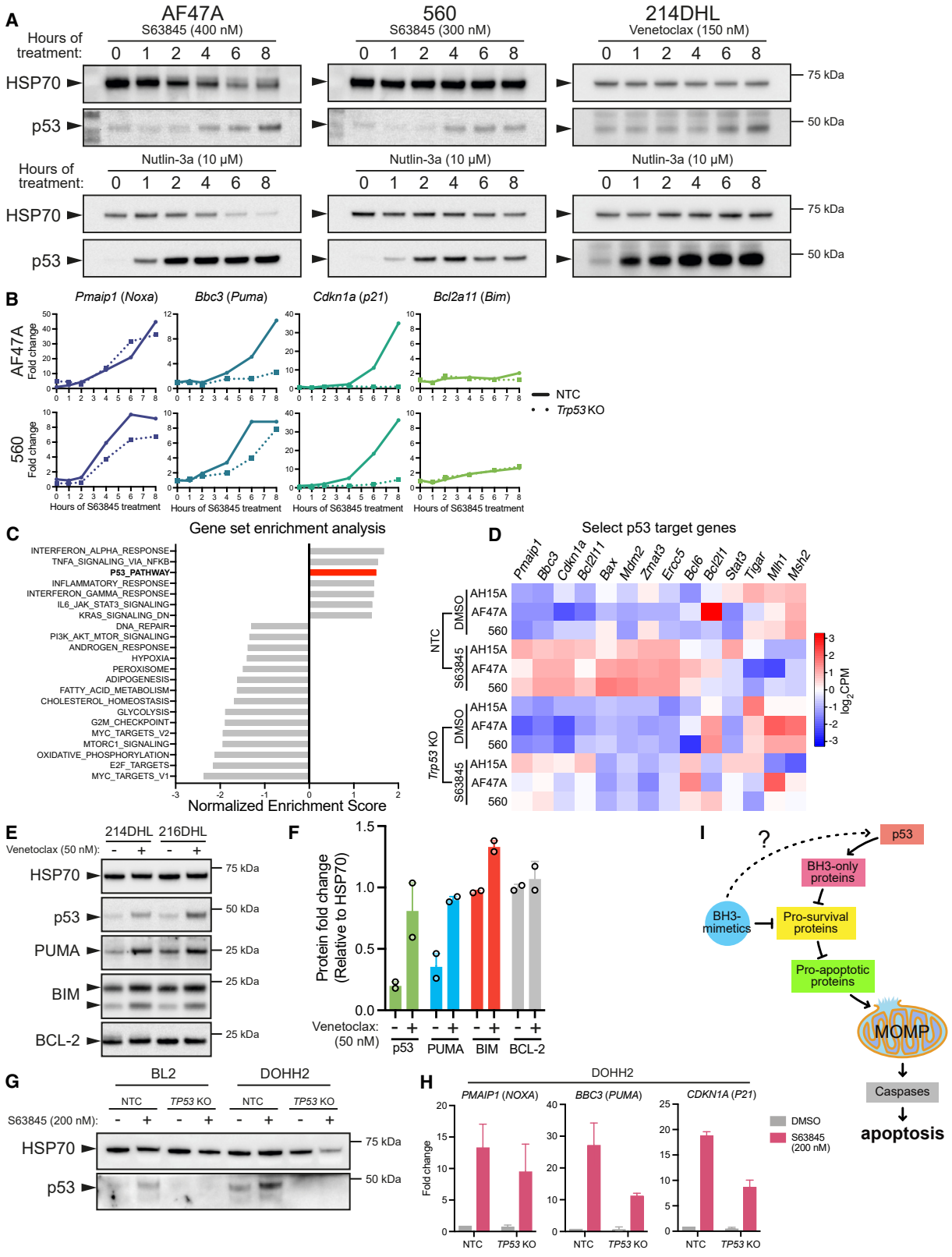

Figure 1. p53 and its downstream target genes are activated by treatment with BH3-mimetics

(A) Immunoblotting of *Eμ-Myc* lymphoma (AF47A/560) and DHL (214DHL) cell lines pre-treated with QVD-*O*-Ph then S63845, venetoclax, or Nutlin-3a for indicated time points. HSP70 was used as a loading control.

(legend continued on next page)

Please cite this article in press as: Diepstraten et al., Putting the STING back into BH3-mimetic drugs for *TP53*-mutant blood cancers, Cancer Cell (2024), https://doi.org/10.1016/j.ccell.2024.04.004

world-wide for treatment of chronic lymphocytic leukemia (CLL) and AML, while BH3-mimetics targeting MCL-1 are in early clinical development.[15–17] Unfortunately, although many patients initially respond well to venetoclax, emerging clinical data suggest that most will relapse.[18,19] A range of resistance mechanisms to BH3-mimetics have been identified[20–25]; perhaps the most surprising being that functional p53 is required for maximal BH3-mimetic drug-induced apoptosis of leukemic cells.[26,27] The mechanisms underlying this p53-mediated response to BH3-mimetic drugs are unclear, but recent analyses show that patients with *TP53*-defective CLL or AML have poorer outcomes after venetoclax treatment than patients with *TP53*-sufficient leukemias.[6,25,28] Ideally, BH3-mimetic therapy would be combined with drugs that can effectively kill malignant cells independently of p53.

Here we report that p53 is activated in lymphoma cells by BH3-mimetic-induced MOMP, and this process induces expression of BH3-only proteins in a feedforward loop, promoting a second wave of apoptosis necessary for maximal cell killing. This feedforward loop is missing in *TP53*-deficient blood cancers, leading to drug resistance. We demonstrate that clinically relevant small molecule stimulator of interferon genes protein (STING) agonists can compensate for loss of *TP53* in a broad range of hematologic cancers by inducing BH3-only protein expression in a cell intrinsic, p53-independent manner. STING is a cytosolic DNA sensor protein best characterized in inflammation and immune stimulation.[29] This new approach repositions STING agonists as a therapeutic drug class with direct and potent oncologic potential against poor prognosis hematologic human cancers in combination with BH3-mimetic drugs.

RESULTS

BH3-mimetic drug treatment causes p53 activation and increased expression of its targets NOXA, PUMA, BIM, and P21

While BH3-mimetic drugs act downstream of p53 to trigger apoptosis, we have previously shown that p53 function is required for maximal apoptosis following BH3-mimetic treatment of leukemia and lymphoma cells.[26] To explore the underlying mechanism, we used cell lines from two independent murine lymphoma models with different BCL-2 pro-survival protein dependencies: the *Eμ-Myc* model of aggressive pre-B/B cell lymphoma,[30,31] which is highly sensitive to BH3-mimetics targeting MCL-1,[32] as well as *Eμ-Myc*-derived double hit lymphoma (DHL) cells, which combines MYC overexpression with pro-survival protein BCL-2 upregulation, and is highly sensitive to BH3-mimetics targeting BCL-2[33] (Figure S1A).

To investigate whether p53 is activated by treatment with BH3-mimetics, we treated *Eμ-Myc* lymphoma and DHL cells with MCL-1 or BCL-2 inhibitors, respectively, and examined p53 expression over time by immunoblotting. As a positive control for potent p53 stabilization/activation, we treated cells with the MDM2 inhibitor Nutlin-3a.[34] We detected p53 protein stabilization in *Eμ-Myc* lymphoma cells (indicative of activation) following 4 h treatment with the MCL-1 inhibitor S63845 (Figure 1A). Similarly, in mouse DHL cells, p53 protein stabilization was evident 6 h post-treatment with the BCL-2 inhibitor venetoclax (Figure 1A). In contrast, p53 protein activation was detected just 1 h after Nutlin-3a treatment in both cell lines, suggesting BH3-mimetics may activate p53 indirectly.

To determine whether the increased p53 protein observed after exposure to BH3-mimetic drugs was functional, *Eμ-Myc* lymphoma cells were treated with an MCL-1 inhibitor and RT-qPCR performed to quantify expression of the direct p53 target genes *Noxa* (*Pmaip1*), *Puma* (*Bbc3*), and *p21* (*Cdkn1a*), and the indirect target gene *Bim* (*Bcl2l11*) (Figure 1B). After S63845 treatment, increased expression of *Noxa*, *Puma*, and *p21* was detected by 4–6 h (Figure 1B). The levels of *Puma* and *p21* were reduced in isogenic variants engineered to be *Trp53* knockout (KO) by CRISPR-Cas9 (cells validated in Figure S1B and a study by Thijssen et al.[26]), demonstrating their induction was largely p53-dependent (Figure 1B). Additionally, we performed RNA sequencing (RNA-seq) analysis on non-targeting single guide (sg)RNA control (NTC) and *Trp53* KO *Eμ-Myc* lymphoma cells treated with S63845 for 24 h. Gene set enrichment analysis (GSEA) of S63845-treated NTC cells demonstrated enrichment of p53 target genes (Figures 1C and S1C), confirming its activation after MCL-1 inhibitor treatment. Of p53 target genes specifically involved in apoptosis, DNA damage repair or metabolism, we identified increased expression of *Pmaip1*/*Noxa*, *Bbc3*/*Puma*, *Cdkn1a*/*p21*, *Bcl2l11*/*Bim*, and *Mdm2*, among others, in NTC cells treated with S63845 (Figures 1D and S1D). This was reduced in *Trp53* KO lymphoma cells (Figures 1D, S1E, and S1F). Similarly, in mouse DHL cells, increased levels of p53, PUMA, and BIM were observed following venetoclax treatment (Figures 1E and 1F). These results demonstrate that p53 is functionally activated after treatment with BH3-mimetics targeting BCL-2 or MCL-1.

To extrapolate this finding to human lymphomas, we generated *TP53*-deficient variants of human diffuse large B cell lymphoma (DLBCL) cell line DOHH2 and Burkitt lymphoma cell line BL2 using CRISPR-Cas9 (Figures S2A and S2B). Analogous to *Eμ-Myc* lymphoma cells, stabilization of p53 protein was observed after S63845 treatment (Figure 1G) and induction of p53 target genes was confirmed in DOHH2 cells, with reduced *PUMA* and *P21* levels observed in their *TP53*-deficient derivatives (Figure 1H).

(B) RT-qPCR for p53 target genes in two independent isogenic non-targeting sgRNA control (NTC) and *Trp53* KO *Eμ-Myc* lymphoma cell lines pre-treated with QVD-*O*-Ph, then S63845 for indicated time points. Fold change is relative to 0 h for each cell line.
(C) RNA-seq GSEA from NTC and *Trp53* KO AH15A, AF47A, and 560 *Eμ-Myc* lymphoma cells pre-treated with QVD-*O*-Ph then 300 nM S63845 for 24 h.
(D) Heatmap of select p53 target genes from experiment in (C).
(E) Immunoblotting of two independent mouse DHL cell lines after pre-treatment with QVD-*O*-Ph then venetoclax for 24 h. HSP70 was used as a loading control.
(F) Quantification of immunoblot in (E).
(G) Immunoblotting of isogenic NTC and *TP53* KO variants of human BL2 and DOHH2 cell lines after pre-treatment with QVD-*O*-Ph then S63845 for 24 h. HSP70 was used as a loading control.
(H) RT-qPCR for p53 target genes in isogenic NTC and *TP53* KO *DOHH2* cell lines pre-treated with QVD-*O*-Ph then S63845 for 24 h. Fold change is shown relative to DMSO-treated NTC cells. Error bars represent SEM for two independent experiments.
(I) Model depicting our observation that BH3-mimetic drug treatment leads to p53 activation. See also Figures S1, S2 and Table S4.

Please cite this article in press as: Diepstraten et al., Putting the STING back into BH3-mimetic drugs for *TP53*-mutant blood cancers, Cancer Cell (2024), https://doi.org/10.1016/j.ccell.2024.04.004

We next examined the role of *Trp53* target genes in resistance to MCL-1 inhibitors. We found that *Noxa*/*Puma*/*Bim*-deficient *Eμ-Myc* lymphoma cells generated by CRISPR-Cas9 (Figure S2C; note, loss of *Noxa* was incomplete in the 560 line)[26] were more resistant to apoptosis than their parental counterparts following treatment with suboptimal doses of S63845, similar to *Trp53* KO cells (Figure S2D). This demonstrates that these pro-apoptotic BH3-only proteins have a major role in the response to BH3-mimetics. To examine the role of p21, we generated *p21*-deficient cells using CRISPR-Cas9 (Figure S2E). All three *p21* KO *Eμ-Myc* lymphoma derivatives had a growth advantage over parental cells in the absence of drug, but an additional advantage during extended culturing with S63845 was only observed in AF47A cells (Figure S2F), suggesting a variable contribution of p21 to cellular responses to MCL-1 inhibitors.

Collectively, these results demonstrate both mouse and human lymphoma cell lines treated with BH3-mimetics can stabilize and functionally activate p53, resulting in p53-dependent transcriptional induction of BH3-only proteins (illustrated in Figure 1I) and augmentation of cell death in response to BH3-mimetics.

p53 is activated by MOMP after treatment with BH3-mimetics

We next sought to determine the underlying mechanism of p53 activation we observed following BH3-mimetic treatment in lymphoma. We have previously shown that BH3-mimetics do not induce DNA damage,[26] effectively ruling out direct DNA damage as the stimulus for our observed p53 activation. To understand the sequence of events preceding p53 activation, we first asked whether p53 activation could occur after MCL-1 inhibition in isogenic *Eμ-Myc* lymphoma cells rendered *Bak*/*Bax*-deficient using CRISPR-Cas9.[20] We found no evidence of increased p53 protein stabilization (Figure 2A), nor of p53 target gene induction post-BH3-mimetic-treatment in the absence of these essential effectors of apoptosis (Figure 2B). Similar results were observed for human NTC and *BAK*/*BAX*-deficient DOHH2 cell lines (Figure 2C), also generated using CRISPR-Cas9 (Figure S3A). As BAK and BAX are essential MOMP effectors in apoptotic cells, our results suggest that MOMP is required for p53 activation following BH3-mimetic treatment (illustrated in Figure 2D).

MOMP induction by sublethal doses of BH3-mimetics has been shown to elicit mitochondrial (mt)DNA release into the cytosol.[13,35] We confirmed this phenomenon occurs in blood cancer cell lines, as cytosolic mtDNA levels were increased 4 h post-treatment with suboptimal BH3-mimetic doses, with no change in cytosolic nuclear DNA detected (Figure S3B). To investigate whether cytosolic mtDNA release was responsible for p53 activation, we derived two independent mtDNA-deficient DOHH2 cell lines (called Rho^0; validated by uridine dependence (Figure S3C) and absent mitochondrial gene expression (Figure S3D)).[36] While we observed a modest trend of reduced induction of *PUMA* and *P21* in these cells following S63845 treatment (Figure S3E), p53 stabilization remained detectable (Figure S3F), indicating that cytosolic mtDNA is not the sole p53 activator post-BH3-mimetic-treatment in these cells. Furthermore, we conclude that caspases must be dispensable for BH3-mimetic-induced p53 activation, as our immunoblotting and RT-qPCR experiments showing p53 activation (Figures 1 and 2) were performed in the presence of caspase inhibitors to facilitate examination of cells that would otherwise undergo demolition.

Activation of the cGAS/STING pathway by BH3-mimetics can induce expression of BH3-only genes, but this is normally silenced by caspases

While examining expression of pro-apoptotic BH3-only genes in lymphoma cells following BH3-mimetic treatment, we observed that although the induction of *Noxa*, *Puma*, and *Bim* was greatly blunted in *Trp53*-deficient cells, it was not abrogated by p53 loss (Figures 1B and 1D). Therefore, we surmised there must also be a p53-independent mechanism promoting BH3-only gene expression following BH3-mimetic treatment. Besides a p53 pathway response, our RNA-seq GSEA analysis of *Eμ-Myc* lymphoma cells treated with S63845 revealed significant enrichment of genes involved in inflammation, interferon signaling and NF-κB signaling (Figure 1C). Release of mtDNA during MOMP has been shown to activate the cytosolic dsDNA-sensing cyclic GMP-AMP synthase/stimulator of interferon genes protein (cGAS/STING) pathway,[37,38] which promotes interferon and NF-κB signaling.[29] In addition, IRF3, a cGAS/STING pathway effector, has been reported to transcriptionally induce expression of BH3-only proteins.[39,40] Therefore, we investigated whether cGAS/STING pathway activation may account for the observed p53-independent induction of BH3-only genes following BH3-mimetic treatment.

We treated isogenic NTC, *Trp53* KO, and *Bak*/*Bax* KO *Eμ-Myc* lymphoma cells with S63845 after QVD-*O*-Ph pre-treatment, and examined expression of phosphorylated (activated) TBK-1 and IRF3, two critical cGAS/STING pathway effectors (Figure S4A). In both NTC and *Trp53* KO cells, TBK-1 and IRF3 phosphorylation was detected, indicating cGAS/STING pathway activation after BH3-mimetic therapy, but this was not observed in *Bak*/*Bax* KO derivatives. These findings confirm that MOMP is required for cGAS/STING pathway activation following BH3-mimetic treatment. We confirmed the *Eμ-Myc* lymphoma lines expressed cGAS, which is necessary for DNA sensing upstream of STING activation (Figure S4B). Phosphorylated (activated) STING was also detectable in NTC and *Trp53* KO *Eμ-Myc* lymphoma cells treated with S63845 in the presence of QVD-*O*-Ph (Figure 3A). We further showed that treatment of mouse DHL cells with venetoclax also led to cGAS/STING pathway activation (Figure 3B), confirming this is a BH3-mimetic class effect.

To determine whether p53-independent expression of *Noxa*, *Puma*, and *Bim* after BH3-mimetic treatment depended upon cGAS/STING pathway activation, we generated *Sting* KO *Eμ-Myc* lymphoma cells using CRISPR-Cas9 (Figure S4C). Notably, p53 was still stabilized and activated in *Sting* KO cells post-treatment with BH3-mimetics, showing that p53 activation is independent of STING (Figure S4D). As expected, activation of STING and its downstream target proteins following MCL-1 inhibition was not observed in *Sting*-deficient *Eμ-Myc* lymphoma cells (Figure 3C). We next examined expression of BH3-only genes in *Eμ-Myc* lymphoma cells treated with QVD-*O*-Ph and S63845 (Figure 3D). In the absence of either *Trp53* or *Sting*, *Noxa*, *Puma*, and *Bim* induction were variably reduced. Simultaneous *Trp53* and *Sting* loss prevented this induction more than loss of either

Please cite this article in press as: Diepstraten et al., Putting the STING back into BH3-mimetic drugs for *TP53*-mutant blood cancers, Cancer Cell (2024), https://doi.org/10.1016/j.ccell.2024.04.004

CellPress
OPEN ACCESS

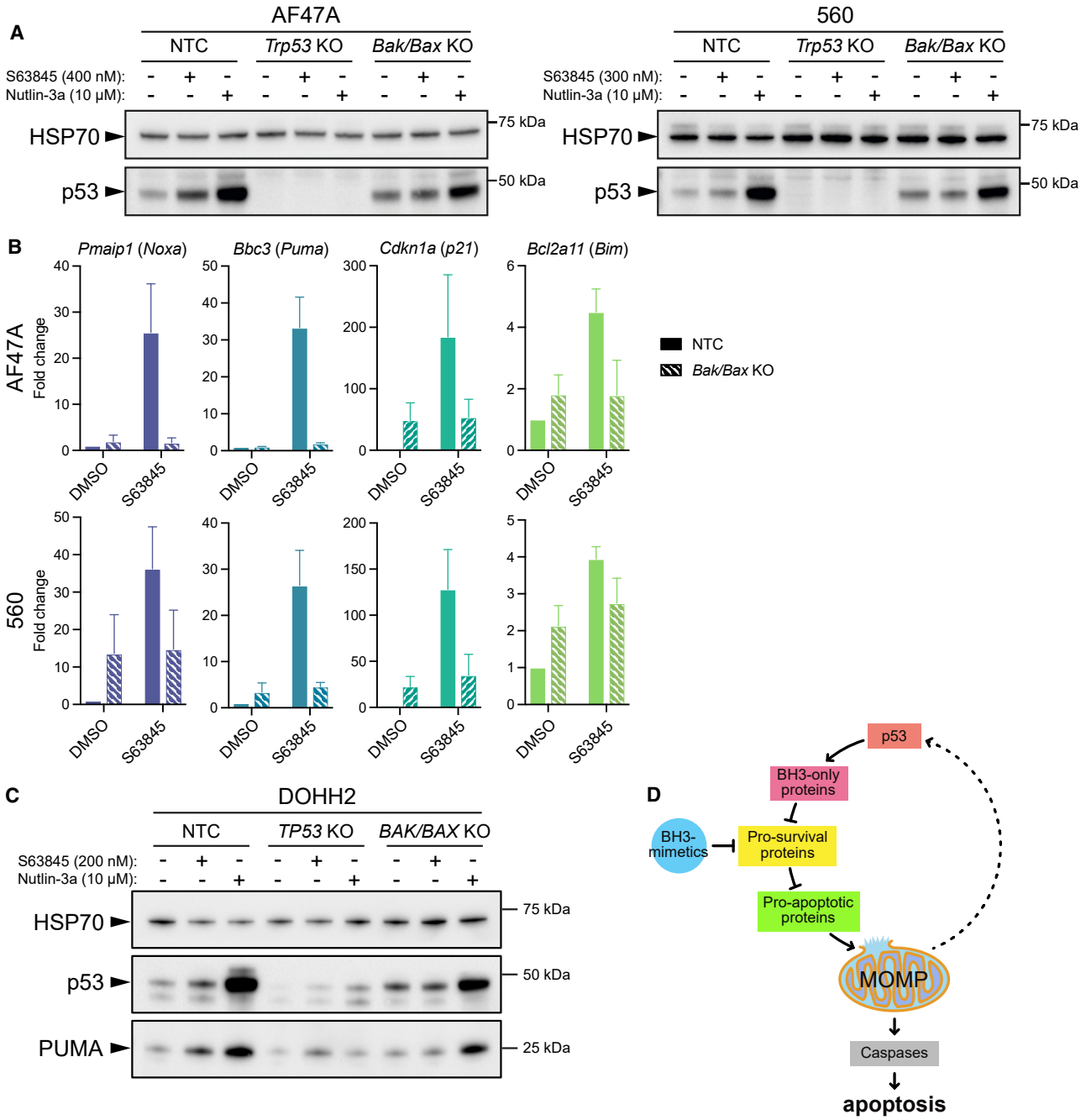

Figure 2. Activation of p53 by BH3-mimetic drugs requires mitochondrial outer membrane permeabilization (MOMP)

(A) Immunoblotting of isogenic non-targeting sgRNA control (NTC), *Trp53* KO, and *Bak/Bax* KO *Eμ-Myc* lymphoma cell lines pre-treated with QVD-*O*-Ph then S63845 or Nutlin-3a for 24 h. HSP70 was used as a loading control.

(B) RT-qPCR for p53 target genes in isogenic NTC and *Bak/Bax* KO *Eμ-Myc* lymphoma cell lines pre-treated with QVD-*O*-Ph then 400 nM (AF47A) or 300 nM (560) S63845 for 24 h. Fold change is relative to DMSO-treated NTC cells. Error bars represent SEM for two independent experiments.

(C) Immunoblotting of isogenic NTC, *TP53* KO, and *BAK/BAX* KO human DOHH2 cells pre-treated with QVD-*O*-Ph then S63845 or Nutlin-3a for 24 h. Blotting for HSP70 was used as a loading control.

(D) Model depicting our observation that MOMP is necessary for BH3-mimetic-mediated p53 activation. See also Figure S3.

gene alone. cGAS/STING pathway activation was also confirmed by increased *Irf7*, *Ifnb1*, *Cxcl10*, and *Ifit1* levels following S63845 treatment in NTC and *Trp53* KO cells, and this was markedly reduced in lymphoma cells lacking STING (Figures 3D, S4E, and S4F). These results demonstrate cGAS/STING signaling can induce p53-independent BH3-only gene expression.

During apoptosis, caspases silence the cGAS/STING pathway to ensure programmed cell death is immunologically

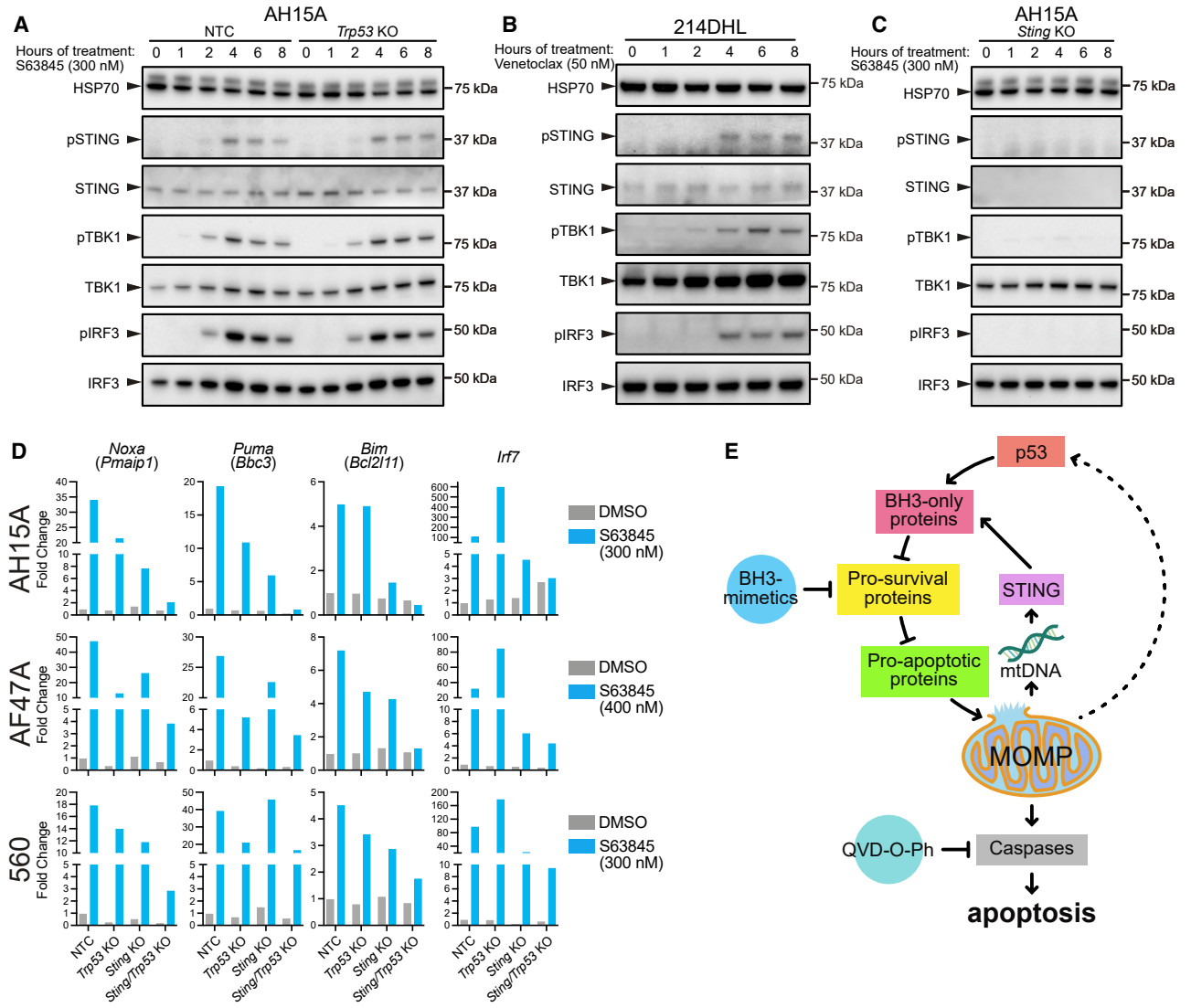

Figure 3. Activation of the cGAS/STING pathway by BH3-mimetic drugs can induce expression of pro-apoptotic BH3-only genes

(A) Immunoblotting for cGAS/STING pathway activation in isogenic NTC and *Trp53* KO *Eμ-Myc* lymphoma cell lines pre-treated with QVD-*O*-Ph then S63845 for the indicated time points. HSP70 was used as a loading control.

(B) Immunoblotting for cGAS/STING pathway activation in 214DHL cells pre-treated with QVD-*O*-Ph then venetoclax for the indicated time points. HSP70 was used as a loading control.

(C) Immunoblotting for cGAS/STING pathway activation in *Sting* KO *Eμ-Myc* lymphoma cells pre-treated with QVD-*O*-Ph then S63845 for the indicated time points. HSP70 was used as a loading control.

(D) RT-qPCR for *Noxa*, *Puma*, *Bim*, and *Irf7* in isogenic NTC, *Trp53* KO, *Sting* KO, and *Trp53*/*Sting* KO *Eμ-Myc* lymphoma cell lines pre-treated with QVD-*O*-Ph then with S63845 for 24 h. Fold change is relative to the DMSO-treated NTC sample. Data shown for three independent *Eμ-Myc* lymphoma cell lines.

(E) Model depicting our observation that in the presence of caspase inhibitors, BH3-mimetic-induced MOMP triggers STING-mediated BH3-only gene expression. See also Figure S4.

silent.[37,38] To permit examination of intact cells after BH3-mimetic treatment, we had conducted our experiments thus far in the presence of caspase inhibitors (QVD-*O*-Ph), which fortuitously enabled cGAS/STING pathway activation to be identified. We hypothesized that the cGAS/STING pathway would not be activated by BH3-mimetics in the absence of caspase inhibitors; however, we could not examine cGAS/STING pathway activation in lymphoma cells post-BH3-mimetic treatment without QVD-*O*-Ph pre-treatment as they are rapidly demolished. Therefore, we performed competition assays comparing NTC and *Sting* KO *Eμ-Myc* lymphoma cells after S63845 treatment without QVD-*O*-Ph (Figure S4G). Two of the three STING-deficient cell lines had a competitive advantage over NTC cells when cultured with DMSO. This suggests that cGAS/STING signaling may contribute to *Eμ-Myc* lymphoma cell death under normal culture conditions in the absence of caspase inhibition. This may relate to the stress imposed by c-MYC overexpression causing a low level of

Please cite this article in press as: Diepstraten et al., Putting the STING back into BH3-mimetic drugs for *TP53*-mutant blood cancers, Cancer Cell (2024), https://doi.org/10.1016/j.ccell.2024.04.004

CellPress
OPEN ACCESS

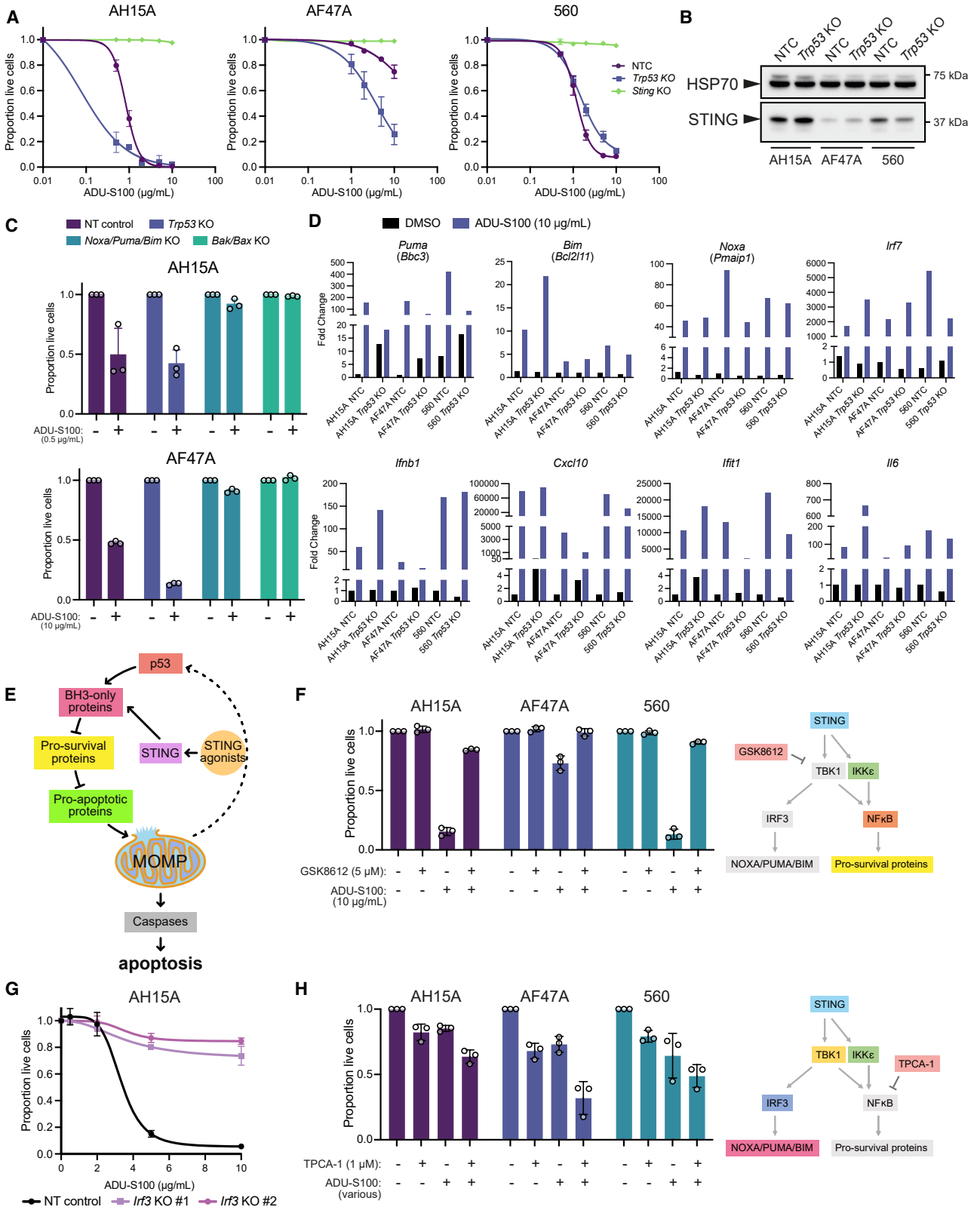

Figure 4. Activation of the cGAS/STING pathway with STING agonists induces apoptosis in mouse *Eμ-Myc* lymphoma cells

(A) Dose-response curves of three independent isogenic NTC, *Trp53* KO, and *Sting* KO *Eμ-Myc* lymphoma cell lines treated with the STING agonist ADU-S100 for 24 h. Error bars represent SD for three independent experiments.

(legend continued on next page)

Please cite this article in press as: Diepstraten et al., Putting the STING back into BH3-mimetic drugs for *TP53*-mutant blood cancers, Cancer Cell (2024), https://doi.org/10.1016/j.ccell.2024.04.004

MOMP that drives cGAS/STING activation. Notably, this effect was not enhanced by S63845 treatment, indicating that cGAS/STING is unlikely to be activated any further by BH3-mimetics without caspase inhibition. Our model of p53-independent STING activation following BH3-mimetic activity is depicted in Figure 3E.

STING agonists induce apoptosis in lymphoma cells by IRF3-mediated activation of PUMA, NOXA, and BIM

To determine if *Eμ-Myc* lymphoma cells could be killed by forced activation of the cGAS/STING pathway, they were treated with ADU-S100, a synthetic cyclic dinucleotide STING agonist currently in clinical trials for solid cancer immune targeting.[41,42] ADU-S100 effectively killed both NTC and *Trp53* KO *Eμ-Myc* lymphoma cells (Figure 4A), and induction of cell death correlated with STING protein levels, but not *Trp53* status (Figure 4B). As expected, STING-deficient cells were unaffected by ADU-S100 (Figure 4A).

To explore how STING agonists induce cell death, *Eμ-Myc* lymphoma cells lacking BAK/BAX were exposed to ADU-S100. BAK/BAX-deficient cells were entirely resistant to STING agonist treatment, demonstrating that these agents kill via apoptosis (Figure 4C). We next examined the effect of ADU-S100 on *Noxa*, *Puma*, and *Bim* induction in *Eμ-Myc* lymphoma cells; all three BH3-only genes were substantially induced in both NTC and *Trp53*-deficient derivative cells, alongside induction of cGAS/STING pathway target genes (Figure 4D). To determine the extent to which STING agonist-mediated cell death was reliant on BH3-only protein induction, we treated *Noxa*/*Puma*/*Bim*-deficient *Eμ-Myc* lymphoma cells with ADU-S100. These triple KO cells were profoundly resistant to STING agonist-mediated killing, demonstrating that these drugs induce BH3-only proteins to trigger apoptosis (Figure 4C). This proposed mechanism is illustrated in Figure 4E.

ADU-S100 is a well-studied STING agonist, but must be delivered intra-tumorally, limiting its clinical utility. Therefore, two additional commercially available small molecule STING agonists were investigated: MSA-2[43] and diABZI compound 3 (also called diABZI STING agonist-1, or diABZI).[44] Both agents induced apoptosis in *Eμ-Myc* lymphoma cells in a NOXA/PUMA/BIM-, BAK/BAX-, and STING-dependent manner (Figures S5A and S5B). Both agents were also less effective in cells with lower levels of STING expression (Figures 4B, S5A and S5B). All STING agonists induced PUMA and BIM protein expression in NTC, *Trp53* KO, and *Bak*/*Bax* KO cells, but not in *Sting* KO cells (Figure S5C). As expected, STING loss did not confer general drug resistance, as *Eμ-Myc* lymphoma cells remained sensitive to doxorubicin, Nutlin-3a, and S63845 (Figure S5D).

Canonical cGAS/STING signaling activates type I interferon (IFN) signaling via IRF3 and NF-κB.[45] To dissect which of these pathways controls STING agonist cytotoxicity, cell death assays were conducted using either IRF3 or NF-κB pathway inhibitors in combination with ADU-S100 or MSA-2. GSK8612 (small molecule TBK1 inhibitor) blocks IRF3 signaling, as although TBK1 promotes activation of both pathways, it is only essential for IRF3 signaling.[45] GSK8612 pre-treatment of *Eμ-Myc* lymphoma cells prevented STING agonist-induced killing, indicating that TBK1/IRF3 signaling is essential for apoptosis (Figures 4F and S5E). Confirming this, *Irf3* KO *Eμ-Myc* lymphoma cells generated by CRISPR-Cas9 (Figure S5F) were resistant to STING agonist-induced killing (Figures 4G and S5G). TPCA-1 (small molecule inhibitor of IKK-2) was employed to suppress NF-κB signaling. As NF-κB signaling can promote pro-survival protein expression,[46] we hypothesized blocking it might enhance lymphoma cell killing by STING agonists. However, only modestly enhanced killing was observed with NF-κB blockade (Figures 4H and S5H). These results identify the essential cGAS/STING pathway components TBK1 and IRF3 as necessary for STING-mediated apoptosis.

Activation of cGAS/STING signaling and type I IFN production may also promote cell-cycle arrest.[47] Although *Bak*/*Bax* KO and *Noxa*/*Puma*/*Bim* KO cells were resistant to diABZI-mediated apoptosis (Figure S5I), proliferation was significantly reduced after 72 h of culture, whereas *Sting* KO cells continued to proliferate normally (Figure S5I). Examining DNA content of *Sting* KO and *Bak*/*Bax* KO cells after 24 h diABZI treatment revealed a trend toward an increased proportion of *Bak*/*Bax* KO cells arrested in G0/G1, whereas no cell-cycle arrest was observed in *Sting* KO lymphoma cells (Figure S5J). These results indicate STING agonists can inhibit lymphoma expansion bimodally; predominantly via apoptosis induction, but also through suppression of proliferation.

Combined BH3-mimetic and STING agonist therapy potently kills *Trp53*-deficient lymphoma cells

To determine whether STING agonists could enhance BH3-mimetic drug activity, particularly against relapse-prone *TP53*-deficient hematological malignancies, NTC and *Trp53* KO *Eμ-Myc* lymphoma cells were treated with S63845 in combination with ADU-S100, MSA-2, or diABZI (Figure 5A). Combination therapy killed NTC and *Trp53* KO lymphoma cells more than either agent alone. *Bak*/*Bax* KO lymphoma cells were entirely

(B) Immunoblotting for baseline STING levels in isogenic NTC and *Trp53* KO *Eμ-Myc* lymphoma cell lines. HSP70 was used as a loading control.
(C) Cell viability assays of two independent isogenic NTC, *Trp53* KO, *Noxa*/*Puma*/*Bim* KO, and *Bak*/*Bax* KO *Eμ-Myc* lymphoma cell lines treated with ADU-S100 for 24 h. Error bars represent SD for three independent experiments.
(D) RT-qPCR for BH3-only and STING target genes in three independent isogenic NTC and *Trp53* KO *Eμ-Myc* lymphoma cell lines treated with ADU-S100 for 24 h. Fold change is relative to the AH15A DMSO-treated NTC sample.
(E) Model depicting our observation that STING agonists induce p53-independent BH3-only gene expression.
(F) Cell viability assays of *Eμ-Myc* lymphoma cell lines treated with ADU-S100 and/or GSK8612 for 24 h. Error bars represent SD for three independent experiments. Diagram illustrates how GSK8612 acts to inhibit TBK1 signaling.
(G) Dose-response curves of isogenic NTC and *Irf3* KO *Eμ-Myc* lymphoma cell lines treated with ADU-S100 for 24 h. Error bars represent SD for two independent experiments.
(H) Cell viability assays of *Eμ-Myc* lymphoma cell lines treated with ADU-S100 (AH15A/560: 0.5 μg/mL; 47A: 5 μg/mL) and/or TPCA-1 for 24 h. Error bars represent SD for three independent experiments. Diagram illustrates how TPCA-1 acts to inhibit NF-κB signaling. See also Figure S5. Statistical comparisons of data presented in this Figure are detailed in Table S4.

Please cite this article in press as: Diepstraten et al., Putting the STING back into BH3-mimetic drugs for *TP53*-mutant blood cancers, Cancer Cell (2024), https://doi.org/10.1016/j.ccell.2024.04.004

CellPress
OPEN ACCESS

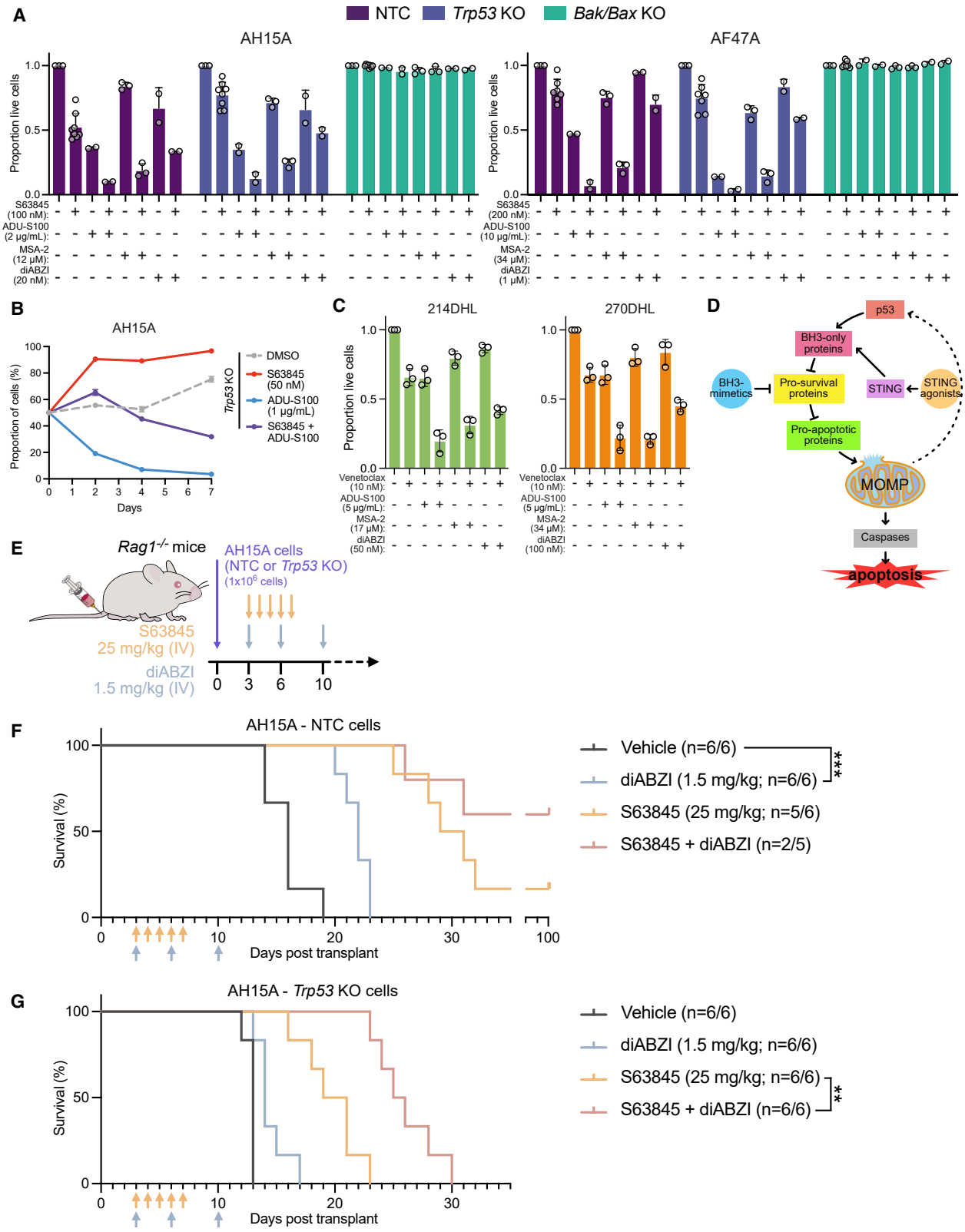

Figure 5. STING agonists combine with BH3-mimetics targeting MCL-1 or BCL-2 to boost apoptosis in mouse *Eμ-Myc* lymphoma cells

(A) Cell viability assays of isogenic NTC, *Trp53* KO, and *Bak*/*Bax* KO *Eμ-Myc* lymphoma cell lines treated with S63845 in combination with ADU-S100, MSA-2, or diABZI for 24 h. Error bars represent SD for at least two independent experiments.

(legend continued on next page)

Please cite this article in press as: Diepstraten et al., Putting the STING back into BH3-mimetic drugs for *TP53*-mutant blood cancers, Cancer Cell (2024), https://doi.org/10.1016/j.ccell.2024.04.004

resistant, confirming this combination therapy relies on apoptosis (Figure 5A). Strikingly, this drug combination effectively suppressed outgrowth of *Trp53* KO over NTC lymphoma cells in competition assays, compared with treatment with BH3-mimetic drugs alone (Figure 5B). Similarly, in mouse DHL cells, additive killing could be achieved by combining a STING agonist with venetoclax (Figure 5C). These results show combining BH3-mimetics with STING agonists can boost apoptosis in *Trp53*-wild-type and *Trp53*-deficient lymphoma cells. A schematic illustrating this enhanced cell killing mechanism is shown in Figure 5D.

We next examined the efficacy and safety of combined BH3-mimetic and STING agonist therapy *in vivo*. STING agonists are being evaluated in clinical trials to boost host immune system stimulation for immunotherapy.[48] However, our data indicated that STING agonists could have a tumor cell-intrinsic effect *in vivo*. To delineate this, NTC or *Trp53* KO *Eμ-Myc* lymphoma cells were transplanted into *Rag1*$^{-/-}$ mice (lacking mature T and B cells). Mice were treated intravenously with S63845, diABZI, or both in combination (Figure 5E). Mice which received NTC lymphoma cells and diABZI alone had significantly longer survival than the vehicle arm (Figure 5F; median survival: 22 days vs. 16 days; $p = 0.0006$). Furthermore, 3/5 mice in the S63845 plus diABZI combination arm remained alive 100 days post-transplantation, compared to only 1/6 mice receiving S63845 monotherapy. For mice transplanted with highly aggressive *Trp53* KO lymphoma cells (Figure 5G), combined S63845 plus diABZI significantly increased survival compared to S63845 alone (median survival: 26 days vs. 20 days; $p = 0.0014$). Blood and tumor-burdened organ analyses confirmed that all mice died from lymphoma (enlarged lymphatic organ(s), increased white blood cells, reduced platelets; Figure S6). These results demonstrate addition of STING agonists to BH3-mimetic therapy can boost killing of *Trp53*-wild-type and *Trp53*-mutant lymphoma cells *in vivo* through cancer cell-intrinsic mechanisms, and tumor-free survival can be prolonged independently of STING agonist effects on immune cells.

STING agonists alone or in combination with MCL-1 inhibitors potently kill lymphoma cells in immune-competent mice

As STING agonists are otherwise being investigated for their immune-promoting properties, we next tested the safety and efficacy of diABZI alone and in combination with S63845 in immune-competent mice transplanted with NTC or *Trp53* KO *Eμ-Myc* lymphoma cells (Figure S7A; note *Cas9* transgenic mice were utilised to avoid rejection of CRISPR/Cas9-modified lymphoma cells). For mice transplanted with NTC cells, treatment with either drug alone or both in combination effectively eliminated all lymphoma cells (Figure S7B). However, in mice transplanted with aggressive *Trp53* KO cells, while S63845 alone did improve survival (median survival: 38 days vs. 13 days; $p = 0.0005$), diABZI alone (5/6 mice lymphoma-free at 150 days) or combined with S63845 (5/5 mice lymphoma-free at 150 days) was highly effective at eliminating *Trp53* KO lymphoma cells (Figure S7C). Blood and organ weight analyses confirmed lymphoma burden at endpoint (Figures S7D and S7E). These results indicate that therapeutic doses of this drug combination are tolerable in immune-competent animals. They also suggest the apoptosis-promoting effects of STING agonists alongside any immune-promoting effects could result in even greater tumor control than appreciated from studies in immune-deficient animals.

STING agonists enhance apoptosis of human ENKTL cells triggered by BH3-mimetics

STING protein expression is necessary for STING agonist function. Therefore, to determine which human blood cancers should be targeted by this approach, *STING* mRNA expression was surveyed in human cancer cell lines from the Cancer Cell Line Encyclopedia (CCLE; Figure S8A). Lymphoma cell lines have dichotomous *STING* expression; low in B cell lymphomas, high in T cell lymphomas. Analysis of STING protein expression in a panel of human B cell lymphoma lines (DLBCL and Burkitt lymphoma) confirmed these cells lacked detectable STING protein (Figure S8B). Consequently, none of these cell lines were sensitive to STING agonist treatment, alone (Figure S8C) or with S63845 (Figure S8D).

In contrast, extranodal NK/T lymphoma (ENKTL) cell lines expressed high levels of STING protein (Figure 6A). Since ENKTLs are highly aggressive with overall poor prognoses, we explored the potential for STING agonists to treat this malignancy. We first generated a *STING*-deficient cell line (MEC04) using CRISPR-Cas9 (Figure S9A). As expected, STING agonists activated cGAS/STING signaling in numerous ENKTL cell lines, but not in MEC04 *STING* KO cells (Figure 6B). Like in mouse lymphoma cells, STING agonists exhibited potent anti-proliferative effects as monotherapies (Figure 6C). It has been reported that ENKTLs rely on BCL-XL for survival,[49] but on-target thrombocytopenia from BCL-XL-targeting BH3-mimetics makes combining these with other, non-platelet-lethal therapies highly desirable. Efficient killing of three p53 pathway-defective ENKTL cell lines, including one with a confirmed *TP53* mutation (MEC04),[49] was achievable by combination treatment with STING agonists and the BCL-XL-targeting BH3-mimetic A-1331852 (Figures 6D and

(B) Cell competition assays of isogenic NTC lymphoma cells vs. their *Trp53* KO derivatives. Lymphoma cells mixed at a 1:1 ratio were treated with DMSO, S63845, ADU-S100, or S63845 and ADU-S100 combined for 7 days, and the proportions of each genotype monitored over time, with the proportions of *Trp53* KO cells plotted. Representative data shown from two independent experiments. Error bars represent SD of two technical replicates.
(C) Cell viability assays of mouse DHL cell lines treated with venetoclax in combination with ADU-S100, MSA-2, or diABZI for 24 h. Data shown for three independent experiments.
(D) Model depicting our observation that BH3-mimetic plus STING agonist combination therapy potently induces apoptosis in lymphoma cells.
(E) Experimental design for *in vivo* treatment of *Rag1*$^{-/-}$ mice bearing transplanted *Eμ-Myc* lymphoma cells. Axis indicates days post-transplant.
(F and G) Survival curves of *Rag1*$^{-/-}$ mice transplanted with isogenic NTC (F) or *Trp53* KO (G) AH15A *Eμ-Myc* lymphoma cells. Arrows indicate when treatments were given. Indicated *n* values are number of mice which reached endpoint due to lymphoma/number of mice included per arm. Note that one mouse from the combination treatment arm in (F) was euthanised at day 3 post-transplant due to illness from an unrelated bacterial infection. This mouse was excluded from analyses. Arms were compared using a log rank Mantel-Cox test with Bonferroni's correction; ** = $p < 0.01$, *** = $p < 0.001$. See also Figures S6, S7, and S12. Statistical comparisons of data presented in this Figure are detailed in Table S4.

Please cite this article in press as: Diepstraten et al., Putting the STING back into BH3-mimetic drugs for *TP53*-mutant blood cancers, Cancer Cell (2024), https://doi.org/10.1016/j.ccell.2024.04.004

CellPress
OPEN ACCESS

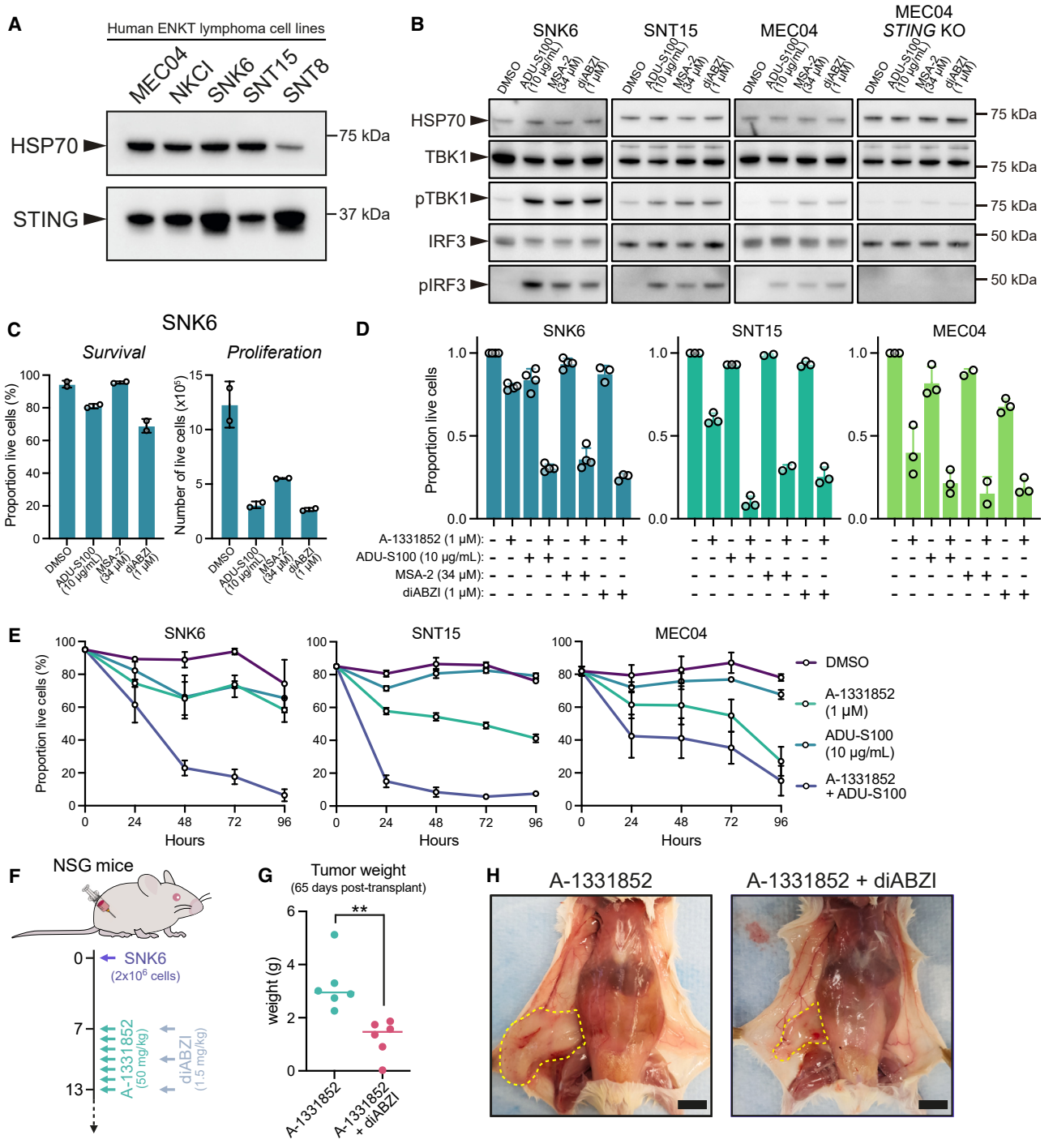

Figure 6. BH3-mimetic drugs targeting BCL-XL combine with STING agonist drugs to boost apoptosis in human ENKTL cell lines

(A) Immunoblotting for STING in a panel of human ENKTL cell lines. HSP70 was used as a loading control.

(B) Immunoblotting for cGAS/STING pathway activation in three independent human ENKTL cell lines (SNK6, SNT15, and MEC04), as well as isogenic MEC04 *STING* KO cells pre-treated with QVD-*O*-Ph then STING agonists for 24 h. HSP70 was used as a loading control.

(C) Cell viability and proliferation of SNK6 cells treated with STING agonists for 72 h. Error bars represent SD for two independent experiments.

(D) Cell viability assays of human ENKTL cell lines treated with A-1331852 in combination with STING agonists for 48 h. Error bars represent SD for at least two independent experiments.

(E) Cell viability assays of ENKTL cell lines treated with A-1331852 in combination with ADU-S100 for the indicated times. Error bars represent SD for two independent experiments.

(F) Experimental design for *in vivo* treatment of *NSG* mice transplanted with SNK6 cells. Axis indicates days post-transplant.

(legend continued on next page)

Please cite this article in press as: Diepstraten et al., Putting the STING back into BH3-mimetic drugs for *TP53*-mutant blood cancers, Cancer Cell (2024), https://doi.org/10.1016/j.ccell.2024.04.004

S9B). This enhanced killing effect increased over time (Figure 6E) but, as expected, was not seen in *STING* KO cells (Figure S9C).

To confirm that STING agonists were inducing pro-apoptotic gene expression in ENKTL cells, we examined *PUMA*, *BIM*, and *NOXA* expression following treatment of three independent cell lines with diABZI, A-1331852, or both drugs in combination (Figure S9D). We observed a marked increase in pro-apoptotic gene expression upon drug combination, with the effect lost in *STING*-deficient cells (Figure S9D). A-1331852 also activated cGAS/STING signaling in the presence of caspase inhibitors (Figure S9E), similar to results for MCL-1 and BCL-2 inhibitors in mouse lymphoma cells (Figures 3A–3C), again confirming this is a class effect of BH3-mimetics.

To test the impact of combined BH3-mimetic and STING agonist therapy on human ENKTLs *in vivo*, NOD-SCID-$\gamma_c^{-/-}$ (NSG) mice were subcutaneously transplanted with SNK6 cells, then treated with either A-1331852 (orally), diABZI (IV), or both drugs in combination (Figure 6F). Small tumors were first detected in mice treated with vehicle or diABZI alone at 32 ± 2 (mean ± SD) or 35 ± 1 day post-transplantation, respectively. Tumors in these mice reached predetermined ethical endpoint volumes at similar times (Figure S9F), with no gross differences between endpoint tumor weights (Figure S9G), lymph node metastases weights (Figure S9H), or blood counts, except for slightly reduced platelet levels in the vehicle-treated mice (Figure S9I). In the A-1331852-treated mice, tumors were first detected 35 ± 2 days post-transplantation, while no tumors were seen in A-1331852 plus diABZI-treated mice until 40 ± 2 days post-transplantation, with 2/6 mice remaining tumor-free until 55 days post-transplantation. The tumors in mice from these two treatment arms eventually grew such that standard external volume estimation was no longer deemed an accurate measure (see STAR methods). Therefore, we sacrificed all mice treated with A-1331852 alone or in combination with diABZI at 65 days post-transplantation, when the first mouse in these arms reached tumor volume ethical endpoint, allowing for direct tumor burden comparisons. We found that primary tumors excised from mice treated with A-1331852 plus diABZI were significantly smaller than those from mice treated with A-1331852 alone (1.3 ± 0.3 g (mean ± SEM) vs. 3 ± 0.4 g, respectively; p = 0.0025; Figures 6G and 6H). Of note, 6/6 mice treated with A-1331852 alone also had an enlarged metastatic proximal axillary lymph node whereas, after combination therapy, 3/6 mice had no evidence of metastasis, and the remaining 3/6 mice exhibited only slight axillary lymph node enlargement (Figure S9J). Blood cell counts from these treatment arms were comparable (Figure S9K). Finally, we observed that 2/6 mice treated with A-1331852 alone had evidence of extensive intra-peritoneal lymphoma, suggesting a more advanced disease, something not observed in any combination treated mice. Overall, these results show that combined BH3-mimetic and STING agonist therapy can suppress outgrowth of aggressive ENKTL cells in mice more potently than either treatment alone, and this is independent of immune effector cell function.

STING agonists enhance killing of human AML cell lines and patient samples targeted by BH3 mimetics

According to CCLE data, myeloid cancer cell lines have the highest *STING* expression among blood cancers (Figure S8A). Therefore, we investigated STING agonist therapy potential for AML. Strong STING protein expression was detected in a panel of *HoxA9/Meis1*-driven mouse AMLs (Figure S10A). Consequently, these cell lines were all effectively killed by diABZI and ADU-S100 (Figure S10B). Turning to human AML, we confirmed robust STING expression in a panel of established cell lines (Figure 7A). As for the lymphoma models with BH3-mimetics, we confirmed that venetoclax treatment activated cGAS/STING signaling in human AML cell lines pre-treated with QVD-*O*-Ph (Figure S10C), indicating that this pathway was functional and targetable in human AMLs. Indeed, all three AML cell lines tested could be efficiently killed by STING agonists as monotherapy (Figure 7B). Consistent with lymphoma cells, isogenic *BAK/BAX*-deficient (Figure S10D) or *STING*-deficient (Figure S10E) AML cells were entirely resistant to killing by diABZI (Figure S10F). Despite increased resistance to venetoclax (Figure S10F), *TP53*-deficient MOLM-13 and MV4;11 cells (engineered by CRISPR-Cas9; Figure S10G) remained highly sensitive to diABZI (Figure S10F). We confirmed that diABZI induced p53-independent expression of *PUMA*, *NOXA*, and *BIM* in AML cells (Figure 7C). Therefore, there is strong rationale to combine STING agonists with venetoclax to enhance killing of *TP53*-mutant AML cells, which respond sub-optimally to BH3-mimetics, even alongside chemotherapy.[15] Indeed, combined STING agonist and venetoclax treatment effectively killed human AML cell lines, regardless of *TP53* status (Figures 7D and S10H).

Moving *in vivo*, we transplanted isogenic MOLM-13 NTC or *TP53* KO cells into NSG mice and treated them with venetoclax, diABZI, or both drugs in combination (Figure 7E). diABZI showed more potent tumor control than venetoclax, in both the NTC (median survival: 24 days vs. 17 days, p = 0.012; Figure 7F) and *TP53* KO cohorts (median survival: 27 days vs. 22 days, p = 0.011; Figure 7G), while mice that received combination therapy survived significantly longer (median survival: 35 days for both NTC and *TP53* KO cohorts) (Figures 7F and 7G). Tumor burden assessment at ethical endpoint confirmed human AML cell outgrowth (Figures S11A and S11B).

We next examined a genomically diverse panel of AML patient samples, including two with *TP53* defects (01-021-2019, 01-058-2023; Figures 8A and S11C; Table S1). Most (4/7) samples were sensitive to diABZI alone, and displayed minimal sensitivity to venetoclax (Figure 8A). The remaining samples (3/7), despite limited sensitivity to diABZI or venetoclax alone, had striking suppression of leukemic blast viability after combined diABZI and venetoclax treatment, a result most prominent in the *TP53*-defective cases (Figure 8A). These results confirm that clinically relevant STING agonists are highly active against primary AML, exerting direct anti-leukemic effects regardless of *TP53* status, and with enhanced activity in combination with venetoclax.

(G) Tumor weights for mice treated with A-1331852, or A-1331852 in combination with diABZI. Lines represent treatment arm median tumor weight at day 65 post-transplantation. 6 mice were included per arm. Student's t test; ** = $p < 0.01$.
(H) Representative tumors (closest to the median weight; yellow outlines) from mice treated with A-1331852, or A-1331852 in combination with diABZI. Scale bars represent 1 cm. See also Figures S8 and S9. Statistical comparisons of data presented in this Figure are detailed in Table S4.

Please cite this article in press as: Diepstraten et al., Putting the STING back into BH3-mimetic drugs for *TP53*-mutant blood cancers, Cancer Cell (2024), https://doi.org/10.1016/j.ccell.2024.04.004

CellPress
OPEN ACCESS

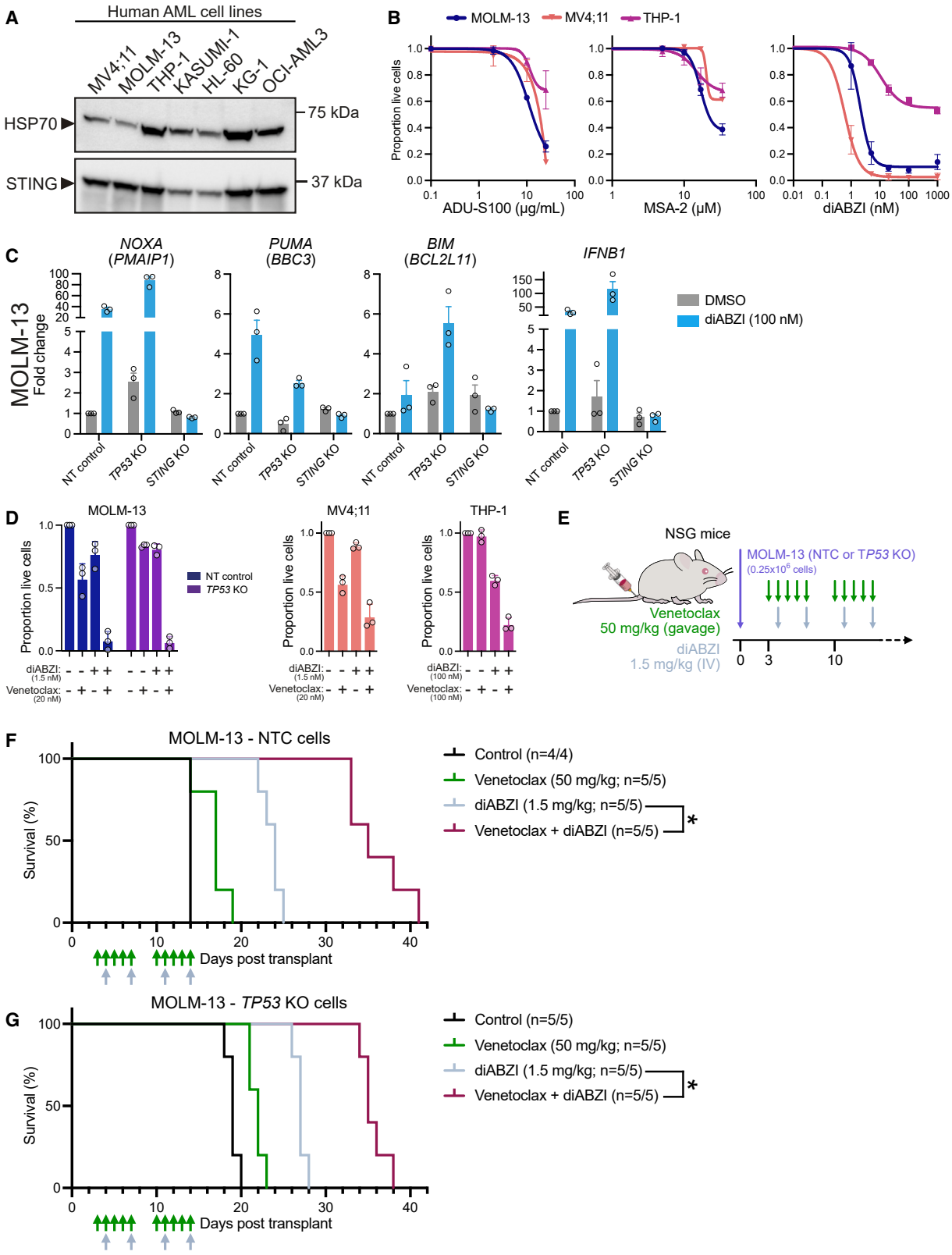

(legend on next page)

Please cite this article in press as: Diepstraten et al., Putting the STING back into BH3-mimetic drugs for *TP53*-mutant blood cancers, Cancer Cell (2024), https://doi.org/10.1016/j.ccell.2024.04.004

Finally, to validate STING agonist impact on primary AML samples *in vivo*, we generated two patient-derived xenograft (PDX) models using highly aggressive relapsed/refractory AML: PDX-1 from a patient with double-hit *TP53*-mutant AML relapsing after venetoclax-based therapy; PDX-2 from a patient refractory to intensive chemotherapy in combination with venetoclax (Table S1). Upon successful engraftment in recipient mice (detectable human CD45$^+$ cells in peripheral blood; Figures S11D and S11E), mice commenced treatment with control, venetoclax alone, diABZI alone, or combination arms (Figure 8B). In both models, diABZI enabled superior survival over venetoclax (*TP53*-mutant PDX-1: median survival: 57.5 vs. 30 days, p = 0.013; Figure 8C; *TP53*-wild-type PDX-2: median survival: 62.5 vs. 38 days, p = 0.012; Figure 8D). In *TP53*-mutant PDX-1, due to its highly aggressive nature, 6/6 control, 5/6 venetoclax, and 1/6 diABZI arm mice reached ethical endpoint before the planned week 2 intra-femoral aspirate to assess disease response (Figure 8E). However, comparing diABZI monotherapy to the diABZI plus venetoclax combination therapy in the remaining mice revealed a greater reduction in leukemic burden in the combination cohort (bone marrow median %hCD45+ cells: 4.6% vs. 0.18%, p = 0.016; Figure 8E). In *TP53*-wild-type PDX-2, the control and venetoclax groups had accumulated a considerable disease burden by week 2 of treatment (bone marrow median % hCD45+ cells: 42.4% vs. 41.6%; Figure 8F). Strikingly, disease burden was greatly reduced by diABZI monotherapy, with a further >10-fold reduction with combination therapy (bone marrow median %hCD45+ cells: 0.46% and 0.03%, respectively; Figure 8F). Human leukemia outgrowth was confirmed at ethical endpoint (Figures S11F and S11G). These results indicate that STING agonists alone or in combination with BH3-mimetics have strong clinical potential in AML, even in *TP53*-mutant disease.

STING agonists alone or in combination with BH3-mimetics are well tolerated by mice, with limited toxicity to healthy human immune cells

We observed no adverse effects in immune-deficient mice treated with STING agonists alone or combined with MCL-1, BCL-2, or BCL-XL inhibitors, nor in immune-competent mice treated with STING agonists alone or combined with MCL-1 inhibitors. Nevertheless, we sought to further characterize potential drug toxicities. First, we assessed potential STING agonist off-target effects. RNA-seq on NTC and *Sting* KO *Eμ-Myc* lymphoma cells pre-treated with QVD-*O*-Ph, then with DMSO or diABZI, revealed 681 genes significantly differentially expressed in NTC cells and 0 in *Sting* KO cells (adj. p value < 0.05, logFC > 0.58), confirming that diABZI specifically activates STING with no detectable off-target effects (Figure S12A).

Next, we assessed STING agonist acute toxicities using immune-competent mice. C57BL/6 mice were treated with diABZI, S63845, venetoclax, each on their own, or diABZI combined with either of these two BH3-mimetics, and peripheral blood cell subsets were examined after 24 h. We found that lymphocytes were depleted by all three drugs as monotherapy, most potently by diABZI (Figure S12B). No major effects on red blood cells, platelets or hematocrit were detected 24 h post-treatment (Figure S12B).

We next investigated the effects of a two-week combination treatment schedule on immune-competent mice (Figure S12C). We observed slight body weight reductions immediately following diABZI administration, but the mice soon recovered (Figure S12D). 96 h after final treatment, mice were euthanized, and bone marrow and peripheral blood examined for immune cell toxicity (Figures S12E and S12F). We noted a slight increase in dendritic cell and granulocyte proportions in the bone marrow, perhaps indicating immune activation by diABZI (Figure S12E). In addition, the proportion of total B cells in the peripheral blood of diABZI-treated mice remained significantly lower than in vehicle-treated mice (Figure S12F). As human B cells express little STING,[50] we expected human B cells to be less impacted by STING agonist therapy than mouse B cells. As predicted, analysis of human blood from healthy donors treated *ex vivo* showed that human T and B cells were resistant to killing by diABZI alone, while NK cells were slightly more sensitive (Figure S13). In comparison, venetoclax appeared more toxic to normal B and NK cells than diABZI alone. Furthermore, healthy T cells were minimally sensitive to diABZI or venetoclax alone, while combined treatment had a greater impact on T and NK cells.

Together, these results identify STING agonists as a promising therapeutic drug class, with potential in patients with STING-expressing blood cancers, and only limited impact on non-malignant blood cells.

DISCUSSION

BH3-mimetic drugs have significantly extended tumor-free survival for several hematological cancers. However, *TP53* mutation is associated with increased relapse risk despite BH3-mimetics inducing apoptosis downstream of p53.[6,25,28] Mechanisms underlying this result were unclear, but we now report that BH3-mimetic-induced MOMP leads to p53 activation. p53 then induces expression of pro-apoptotic BH3-only proteins, a

Figure 7. STING agonists combine with BH3-mimetics targeting BCL-2 to boost apoptosis in AML cell lines *in vitro* and in xenograft models

(A) Immunoblotting for STING in a panel of human AML cell lines. HSP70 was used as a loading control.

(B) Dose-response curves of MOLM-13 (*TP53*-wild-type), MV4;11 (*TP53*-wild-type), and THP-1 (*TP53*-mutant) cells treated with STING agonists for 24 h. Error bars represent SD for two independent experiments.

(C) RT-qPCR for *NOXA*, *PUMA*, *BIM*, and *IFNB1* in isogenic NTC, *Trp53* KO, and *STING* KO MOLM-13 cell lines treated with diABZI for 24 h. Fold change is relative to the DMSO-treated NTC sample. Error bars represent SEM for three independent experiments.

(D) Cell viability assays of human AML cell lines treated with venetoclax in combination with diABZI for 24 h. Error bars represent SD for three independent experiments.

(E) Experimental design for *in vivo* treatment of NSG mice transplanted with MOLM-13 human AML cells. Axis indicates days post-transplant.

(F and G) Survival curves of NSG mice transplanted with isogenic NTC (F) or *TP53* KO (G) MOLM-13 human AML cells. Arrows indicate when treatments were given. Indicated n values are number of mice which reached endpoint due to leukemia/total number of mice included per arm. Arms were compared using a log rank Mantel-Cox test with Bonferroni's correction; * = $p < 0.05$. See also Figures S10 and S11. Statistical comparisons of data presented in this Figure are detailed in Table S4.

Please cite this article in press as: Diepstraten et al., Putting the STING back into BH3-mimetic drugs for *TP53*-mutant blood cancers, Cancer Cell (2024), https://doi.org/10.1016/j.ccell.2024.04.004

CellPress
OPEN ACCESS

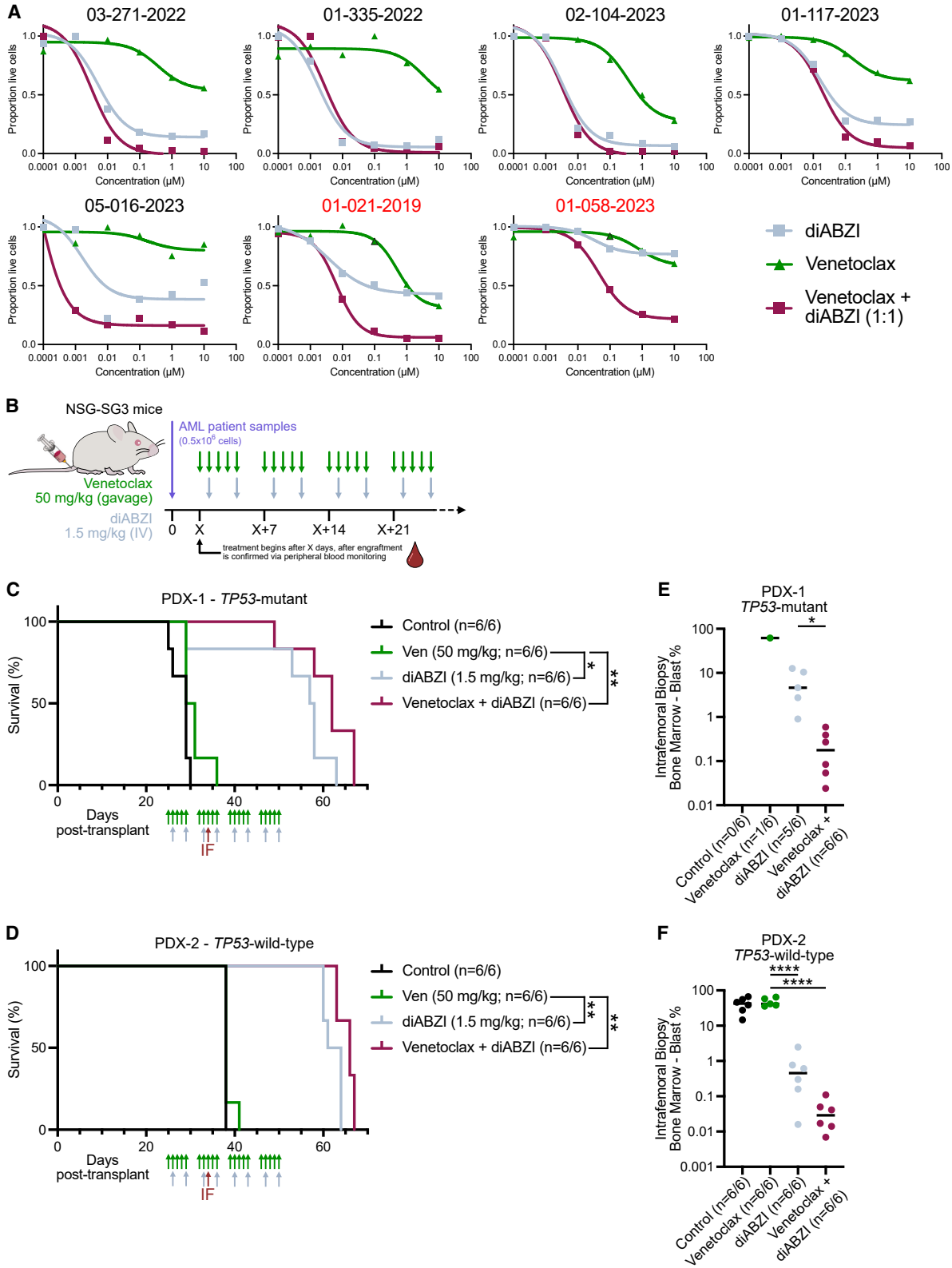

(legend on next page)

feedforward loop that augments the death of malignant cells that otherwise might not reach the necessary apoptotic threshold. Importantly, this occurred with both MCL-1 and BCL-2 inhibitors, suggesting it is a BH3-mimetic class effect. This new facet of p53-mediated tumor suppression, where it not only triggers but enforces apoptosis, may have implications for other drugs that endeavor to trigger apoptosis downstream of p53. Future investigations in other cancer types or non-transformed cells will provide important insights into this potential new tumor-suppressive function of p53.

Armed with an understanding of the requirements to efficiently induce apoptosis in *TP53*-mutant blood cancer cells, we identified that cGAS/STING pathway activation can boost pro-apoptotic BH3-only protein expression in a p53-independent manner. STING agonists are in clinical trials in combination with immunotherapy, aiming to enhance host anti-cancer immune responses.[48,51] These studies have so far reported limited efficacy from stimulation of the host immune response by STING agonists,[48,51] but have critically demonstrated the tolerability of these drugs in humans, with the main adverse events relating to consequences of cytokine release.[52,53] In this study, we repurposed this drug class and showed that both synthetic cyclic dinucleotide and small molecule STING agonists could kill mouse and human blood cancer cells directly, triggering tumor cell-intrinsic apoptosis *in vitro* and *in vivo*, without the requirement of immune activation. The extent of cell killing was *TP53* status agnostic but required STING protein. Stringent characterization of this pathway revealed that the TBK1/IRF3 axis was essential for killing, while NF-κB signaling was dispensable (though not antagonistic). Understanding the critical regulators required for apoptotic induction by cGAS/STING signaling not only assists with patient selection, but exposes the pathway to further manipulation to improve pro-apoptotic STING signaling in future.

Importantly, we demonstrate that combining STING agonists with BH3-mimetics can boost apoptosis in both *TP53*/*TRP53*-wild-type and *TP53*/*TRP53*-mutant leukemias and lymphomas. STING agonists alone or in combination with venetoclax were highly efficacious in AML patient samples and PDX models, regardless of *TP53* status, even in samples insensitive to venetoclax alone. In human ENKTL, the combination of BCL-XL inhibition and STING agonists potently killed malignant cells with non-functional p53. Crucially, the combination of BH3-mimetics with STING agonists was well tolerated in immune-competent mice, even those bearing aggressive lymphomas. ENKTL[54] and *TP53*-mutant AML[55] represent two blood cancer subtypes with limited therapy options and dismal prognoses. As both BH3-mimetic and STING agonist drugs are already in clinical trials (or widely approved and used, in the case of venetoclax), this drug combination could be fast-tracked to the clinic for immediate translational impact.

STAR★METHODS

Detailed methods are provided in the online version of this paper and include the following:

- KEY RESOURCES TABLE
- RESOURCE AVAILABILITY
  - Lead contact
  - Materials availability
  - Data and code availability
- EXPERIMENTAL MODEL AND STUDY PARTICIPANT DETAILS
  - Cancer cell lines and tissue culture
  - Primary AML and healthy donor specimens
  - Mice
- METHOD DETAILS
  - *Eμ-Myc* lymphoma mouse experiments
  - Human ENKT lymphoma xenograft experiments
  - Human AML xenograft mouse experiments
  - Drug toxicity experiments in mice
  - CRISPR-Cas9 gene knockout cell lines
  - Next generation sequencing
  - Cell line death assays
  - Primary specimen death assays
  - Immunoblotting
  - Quantitative reverse transcriptase PCR
  - RNA-seq of *Eμ-Myc* lymphoma cells
  - Generation and culture of mouse AML cells
  - Cell cycle and proliferation analyses
  - Rho^0 cells and cytosolic mtDNA analysis
  - Imaging
- QUANTIFICATION AND STATISTICAL ANALYSIS

SUPPLEMENTAL INFORMATION

Supplemental information can be found online at https://doi.org/10.1016/j.ccell.2024.04.004.

ACKNOWLEDGMENTS

We thank WEHI colleagues for support and advice, particularly Elizabeth Lieschke, Yexuan Deng, Margaret Potts, Christina Koenig, Lin Tai, and Marco Herold; Duong Nhu and Guillaume Lessene for A-1331852; WEHI Bioservices, particularly Lauren Wilkins, Natasha Blasch, Natalia MoraTorres and Giovanni Siciliano; the WEHI FACS team and professional services; and the patients who donated their samples for research.

This study was supported by the Australian Government NHMRC (GNT1113133 [A.S.], GNT1116937 [A.S.], GNT2018071 [A.H.W.], GNT2002618 [G.L.K.], GNT2001201 [G.L.K.], GNT2011139 [G.L.K., A.W.R.,

Figure 8. STING agonists combine with BH3-mimetic drugs targeting BCL-2 to boost apoptosis in human AML patient samples and patient-derived xenograft (PDX) models

(A) Cell viability assays of leukemic blasts (CD117+) from seven independent human AML patient samples following 48 h of indicated treatment. *TP53*-mutant samples are labeled in red.

(B) Experimental design for *in vivo* treatment of AML PDX models in *NSG-SG3* mice.

(C and D) Survival curves of *TP53*-mutant (C) or *TP53*-wild-type (D) AML PDX models. Arrows indicate when treatments were given. IF indicates when intra-femoral biopsies were performed. Indicated *n* values are number of mice which reached ethical endpoint due to leukemia/total number of mice included in arm. Arms were compared using a log rank Mantel-Cox test with Bonferroni's correction; * = $p < 0.05$, ** = $p < 0.01$.

(E and F) Intra-femoral biopsy on *TP53*-mutant (E) and *TP53*-wild-type (F) PDX mice. Indicated *n* values are number of mice alive at time of biopsy/total number of mice included per arm. Lines represent mean measurements. Treatment groups (diABZI and venetoclax/diABZI) in PDX-1 (E) were compared using Student's t test; * = $p < 0.05$. Arms in PDX-2 (F) were compared using a one-way ANOVA with Tukey's multiple comparisons; ** = $p < 0.01$, *** = $p < 0.001$, **** = $p < 0.0001$. See also Figures S11 and S13, Table S1.

and A.H.W.], GNT2010275 [A.S.], GNT1176175 [F.C.B.], GNT1174902 [A.W.R.], and GNT2014234 [Y.Y.]), Victorian Cancer Agency (17028 [G.L.K.] and 21006 [S.T.D.]), MRFF (2023403 [A.H.W.]), CASS Foundation (S.T.D. and J.E.L.M.), estate of Anthony (Toni) Redstone OAM (A.S. and G.L.K.), Craig Perkins Cancer Research Foundation (G.L.K.), Dyson Bequest (G.L.K.), Harry Secomb Foundation (G.L.K.), Robert and Janette Boffey (J.E.L.M.), Jill and Stuart Bales (S.T.D.), Metcalf Family Fellowship (A.H.W.), RCPA Foundation (Y.Y), and the Victorian State Government Operational Infrastructure Support and NHMRC Independent Research Institute Infrastructure Support schemes.

AUTHOR CONTRIBUTIONS

Conceptualization: G.L.K., S.T.D., and A.S. Supervision of study: G.L.K. Mouse/human B cell and ENKTL experiments: S.T.D. with assistance from J.E.L.M. and S.Y. Mouse AML experiments: J.E.L.M. with assistance from C.C. and K.C.F. Mouse toxicity experiments: A.M.R. and L.W. with assistance from S.Y., S.T.D., and C.C. *In vivo* lymphoma experiments: S.T.D. and L.W. with assistance from J.E.L.M. and S.Y. Human AML experiments: S.T.D. and Y.Y. with assistance from K.C.F., R.M., G.P., A.G., F.C.B., and A.W.H. Primary human sample experiments: Y.Y., F.C.B., and A.H.W. *In vivo* AML experiments: V.L., Y.Y., and F.C.B. Student supervision: A.H.W., A.W.R., and F.C.B. Manuscript draft: S.T.D. Figure preparation: S.T.D. and J.E.L.M. Manuscript revision: S.T.D., J.E.L.M., G.L.K., A.S., and A.H.W. All authors reviewed and approved the manuscript.

DECLARATION OF INTERESTS

All authors are employees of WEHI which receives milestone and royalty payments related to venetoclax. A.S., A.H.W., and G.L.K. have in the past received research funding from Servier for work on the development of MCL-1 inhibitors. A.W.R. has previously received research funding from AbbVie and is an inventor on a patent related to venetoclax dosing. A.H.W. has received research funding from AbbVie and consulting fees from AbbVie for clinical trials related to venetoclax. We have submitted a provisional patent application to cover the rationale of the described drug combination (STING agonists alongside BH3-mimetics).

Received: July 23, 2023
Revised: January 6, 2024
Accepted: April 4, 2024
Published: April 25, 2024

REFERENCES

1. Stanchina, M., Soong, D., Zheng-Lin, B., Watts, J.M., and Taylor, J. (2020). Advances in Acute Myeloid Leukemia: Recently Approved Therapies and Drugs in Development. Cancers *12*, e3225. https://doi.org/10.3390/cancers12113225.
2. Yosifov, D.Y., Wolf, C., Stilgenbauer, S., and Mertens, D. (2019). From Biology to Therapy: The CLL Success Story. Hemasphere *3*, e175. https://doi.org/10.1097/hs9.0000000000000175.
3. Zenz, T., Kreuz, M., Fuge, M., Klapper, W., Horn, H., Staiger, A.M., Winter, D., Helfrich, H., Huellein, J., Hansmann, M.L., et al. (2017). TP53 mutation and survival in aggressive B cell lymphoma. Int. J. Cancer *141*, 1381–1388. https://doi.org/10.1002/ijc.30838.
4. Zenz, T., Eichhorst, B., Busch, R., Denzel, T., Häbe, S., Winkler, D., Bühler, A., Edelmann, J., Bergmann, M., Hopfinger, G., et al. (2010). TP53 mutation and survival in chronic lymphocytic leukemia. J. Clin. Oncol. *28*, 4473–4479. https://doi.org/10.1200/JCO.2009.27.8762.
5. Stengel, A., Kern, W., Haferlach, T., Meggendorfer, M., Fasan, A., and Haferlach, C. (2017). The impact of TP53 mutations and TP53 deletions on survival varies between AML, ALL, MDS and CLL: an analysis of 3307 cases. Leukemia *31*, 705–711. https://doi.org/10.1038/leu.2016.263.
6. Pollyea, D.A., Pratz, K.W., Wei, A.H., Pullarkat, V., Jonas, B.A., Recher, C., Babu, S., Schuh, A.C., Dail, M., Sun, Y., et al. (2022). Outcomes in Patients with Poor-Risk Cytogenetics with or without TP53 Mutations Treated with Venetoclax and Azacitidine. Clin. Cancer Res. *28*, 5272–5279. https://doi.org/10.1158/1078-0432.Ccr-22-1183.
7. Marei, H.E., Althani, A., Afifi, N., Hasan, A., Caceci, T., Pozzoli, G., Morrione, A., Giordano, A., and Cenciarelli, C. (2021). p53 signaling in cancer progression and therapy. Cancer Cell Int. *21*, e703. https://doi.org/10.1186/s12935-021-02396-8.
8. Grob, T., Al Hinai, A.S.A., Sanders, M.A., Kavelaars, F.G., Rijken, M., Gradowska, P.L., Biemond, B.J., Breems, D.A., Maertens, J., van Marwijk Kooy, M., et al. (2022). Molecular characterization of mutant TP53 acute myeloid leukemia and high-risk myelodysplastic syndrome. Blood *139*, 2347–2354. https://doi.org/10.1182/blood.2021014472.
9. de Mel, S., Hue, S.S.-S., Jeyasekharan, A.D., Chng, W.-J., and Ng, S.-B. (2019). Molecular pathogenic pathways in extranodal NK/T cell lymphoma. J. Hematol. Oncol. *12*, 33. https://doi.org/10.1186/s13045-019-0716-7.
10. Aubrey, B.J., Kelly, G.L., Janic, A., Herold, M.J., and Strasser, A. (2018). How does p53 induce apoptosis and how does this relate to p53-mediated tumour suppression? Cell Death Differ. *25*, 104–113. https://doi.org/10.1038/cdd.2017.169.
11. Vitale, I., Pietrocola, F., Guilbaud, E., Aaronson, S.A., Abrams, J.M., Adam, D., Agostini, M., Agostinis, P., Alnemri, E.S., Altucci, L., et al. (2023). Apoptotic cell death in disease—Current understanding of the NCCD 2023. Cell Death Differ. *30*, 1097–1154. https://doi.org/10.1038/s41418-023-01153-w.
12. Kalkavan, H., Chen, M.J., Crawford, J.C., Quarato, G., Fitzgerald, P., Tait, S.W.G., Goding, C.R., and Green, D.R. (2022). Sublethal cytochrome c release generates drug-tolerant persister cells. Cell *185*, 3356–3374.e22. https://doi.org/10.1016/j.cell.2022.07.025.
13. Ichim, G., Lopez, J., Ahmed, S.U., Muthalagu, N., Giampazolias, E., Delgado, M.E., Haller, M., Riley, J.S., Mason, S.M., Athineos, D., et al. (2015). Limited mitochondrial permeabilization causes DNA damage and genomic instability in the absence of cell death. Mol. Cell. *57*, 860–872. https://doi.org/10.1016/j.molcel.2015.01.018.
14. Dörflinger, B., Badr, M.T., Haimovici, A., Fischer, L., Vier, J., Metz, A., Eisele, B., Bronsert, P., Aumann, K., Höppner, J., et al. (2022). Mitochondria supply sub-lethal signals for cytokine secretion and DNA-damage in H. pylori infection. Cell Death Differ. *29*, 2218–2232. https://doi.org/10.1038/s41418-022-01009-9.
15. Diepstraten, S.T., Anderson, M.A., Czabotar, P.E., Lessene, G., Strasser, A., and Kelly, G.L. (2022). The manipulation of apoptosis for cancer therapy using BH3-mimetic drugs. Nat. Rev. Cancer *22*, 45–64. https://doi.org/10.1038/s41568-021-00407-4.
16. Roberts, A.W., Davids, M.S., Pagel, J.M., Kahl, B.S., Puvvada, S.D., Gerecitano, J.F., Kipps, T.J., Anderson, M.A., Brown, J.R., Gressick, L., et al. (2016). Targeting BCL2 with venetoclax in relapsed chronic lymphocytic leukemia. N. Engl. J. Med. *374*, 311–322. https://doi.org/10.1056/NEJMoa1513257.
17. DiNardo, C.D., Jonas, B.A., Pullarkat, V., Thirman, M.J., Garcia, J.S., Wei, A.H., Konopleva, M., Döhner, H., Letai, A., Fenaux, P., et al. (2020). Azacitidine and Venetoclax in Previously Untreated Acute Myeloid Leukemia. N. Engl. J. Med. *383*, 617–629. https://doi.org/10.1056/NEJMoa2012971.
18. Anderson, M.A., Tam, C., Lew, T.E., Juneja, S., Juneja, M., Westerman, D., Wall, M., Lade, S., Gorelik, A., Huang, D.C.S., et al. (2017). Clinicopathological features and outcomes of progression of CLL on the BCL2 inhibitor venetoclax. Blood *129*, 3362–3370. https://doi.org/10.1182/blood-2017-01-763003.
19. Maiti, A., Rausch, C.R., Cortes, J.E., Pemmaraju, N., Daver, N.G., Ravandi, F., Garcia-Manero, G., Borthakur, G., Naqvi, K., Ohanian, M., et al. (2021). Outcomes of relapsed or refractory acute myeloid leukemia after frontline hypomethylating agent and venetoclax regimens. Haematologica *106*, 894–898. https://doi.org/10.3324/haematol.2020.252569.
20. Diepstraten, S.T., Young, S., La Marca, J.E., Wang, Z., Kluck, R.M., Strasser, A., and Kelly, G.L. (2023). Lymphoma cells lacking pro-apoptotic BAX are highly resistant to BH3-mimetics targeting pro-survival MCL-1

but retain sensitivity to conventional DNA-damaging drugs. Cell Death Differ. *30*, 1005–1017. https://doi.org/10.1038/s41418-023-01117-0.

21. Thomalla, D., Beckmann, L., Grimm, C., Oliverio, M., Meder, L., Herling, C.D., Nieper, P., Feldmann, T., Merkel, O., Lorsy, E., et al. (2022). Deregulation and epigenetic modification of BCL2-family genes cause resistance to venetoclax in hematologic malignancies. Blood *140*, 2113–2126. https://doi.org/10.1182/blood.2021014304.
22. Moujalled, D.M., Brown, F.C., Chua, C.C., Dengler, M.A., Pomilio, G., Anstee, N.S., Litalien, V., Thompson, E., Morley, T., MacRaild, S., et al. (2023). Acquired mutations in BAX confer resistance to BH3-mimetic therapy in Acute Myeloid Leukemia. Blood *141*, 634–644. https://doi.org/10.1182/blood.2022016090.
23. Thijssen, R., Tian, L., Anderson, M.A., Flensburg, C., Jarratt, A., Garnham, A.L., Jabbari, J.S., Peng, H., Lew, T.E., Teh, C.E., et al. (2022). Single-cell multiomics reveal the scale of multilayered adaptations enabling CLL relapse during venetoclax therapy. Blood *140*, 2127–2141. https://doi.org/10.1182/blood.2022016040.
24. Blombery, P., Lew, T.E., Dengler, M.A., Thompson, E.R., Lin, V.S., Chen, X., Nguyen, T., Panigrahi, A., Handunnetti, S.M., Carney, D.A., et al. (2022). Clonal hematopoiesis, myeloid disorders and BAX-mutated myelopoiesis in patients receiving venetoclax for CLL. Blood *139*, 1198–1207. https://doi.org/10.1182/blood.2021012775.
25. DiNardo, C.D., Tiong, I.S., Quaglieri, A., MacRaild, S., Loghavi, S., Brown, F.C., Thijssen, R., Pomilio, G., Ivey, A., Salmon, J.M., et al. (2020). Molecular patterns of response and treatment failure after frontline venetoclax combinations in older patients with AML. Blood *135*, 791–803. https://doi.org/10.1182/blood.2019003988.
26. Thijssen, R., Diepstraten, S.T., Moujalled, D., Chew, E., Flensburg, C., Shi, M.X., Dengler, M.A., Litalien, V., MacRaild, S., Chen, M., et al. (2021). Intact TP-53 function is essential for sustaining durable responses to BH3-mimetic drugs in leukemias. Blood *137*, 2721–2735. https://doi.org/10.1182/blood.2020010167.
27. Nechiporuk, T., Kurtz, S.E., Nikolova, O., Liu, T., Jones, C.L., D'Alessandro, A., Culp-Hill, R., d'Almeida, A., Joshi, S.K., Rosenberg, M., et al. (2019). The TP53 Apoptotic Network Is a Primary Mediator of Resistance to BCL2 Inhibition in AML Cells. Cancer Discov. *9*, 910–925. https://doi.org/10.1158/2159-8290.CD-19-0125.
28. Roberts, A.W., Ma, S., Kipps, T.J., Coutre, S.E., Davids, M.S., Eichhorst, B., Hallek, M., Byrd, J.C., Humphrey, K., Zhou, L., et al. (2019). Efficacy of venetoclax in relapsed chronic lymphocytic leukemia is influenced by disease and response variables. Blood *134*, 111–122. https://doi.org/10.1182/blood.2018882555.
29. Motwani, M., Pesiridis, S., and Fitzgerald, K.A. (2019). DNA sensing by the cGAS-STING pathway in health and disease. Nat. Rev. Genet. *20*, 657–674. https://doi.org/10.1038/s41576-019-0151-1.
30. Adams, J.M., Harris, A.W., Pinkert, C.A., Corcoran, L.M., Alexander, W.S., Cory, S., Palmiter, R.D., and Brinster, R.L. (1985). The *c-myc* oncogene driven by immunoglobulin enhancers induces lymphoid malignancy in transgenic mice. Nature *318*, 533–538. https://doi.org/10.1038/318533a0.
31. Harris, A.W., Pinkert, C.A., Crawford, M., Langdon, W.Y., Brinster, R.L., and Adams, J.M. (1988). The Eμ-*myc* transgenic mouse: a model for high-incidence spontaneous lymphoma and leukemia of early B cells. J. Exp. Med. *167*, 353–371. https://doi.org/10.1084/jem.167.2.353.
32. Kotschy, A., Szlavik, Z., Murray, J., Davidson, J., Maragno, A.L., Le Toumelin-Braizat, G., Chanrion, M., Kelly, G.L., Gong, J.N., Moujalled, D.M., et al. (2016). The MCL1 inhibitor S63845 is tolerable and effective in diverse cancer models. Nature *538*, 477–482. https://doi.org/10.1038/nature19830.
33. Deng, Y., Diepstraten, S.T., Potts, M.A., Giner, G., Trezise, S., Ng, A.P., Healey, G., Kane, S.R., Cooray, A., Behrens, K., et al. (2022). Generation of a CRISPR activation mouse that enables modelling of aggressive lymphoma and interrogation of venetoclax resistance. Nat. Commun. *13*, e4739. https://doi.org/10.1038/s41467-022-32485-9.
34. Vassilev, L.T., Vu, B.T., Graves, B., Carvajal, D., Podlaski, F., Filipovic, Z., Kong, N., Kammlott, U., Lukacs, C., Klein, C., et al. (2004). In Vivo Activation of the p53 Pathway by Small-Molecule Antagonists of MDM2. Science *303*, 844–848. https://doi.org/10.1126/science.1092472.
35. Riley, J.S., Quarato, G., Cloix, C., Lopez, J., O'Prey, J., Pearson, M., Chapman, J., Sesaki, H., Carlin, L.M., Passos, J.F., et al. (2018). Mitochondrial inner membrane permeabilisation enables mtDNA release during apoptosis. EMBO J. *37*, e99238. https://doi.org/10.15252/embj.201899238.
36. King, M.P., and Attardi, G. (1989). Human cells lacking mtDNA: repopulation with exogenous mitochondria by complementation. Science *246*, 500–503. https://doi.org/10.1126/science.2814477.
37. White, M.J., McArthur, K., Metcalf, D., Lane, R.M., Cambier, J.C., Herold, M.J., van Delft, M.F., Bedoui, S., Lessene, G., Ritchie, M.E., et al. (2014). Apoptotic caspases suppress mtDNA-induced STING-mediated type I IFN production. Cell *159*, 1549–1562. https://doi.org/10.1016/j.cell.2014.11.036.
38. Rongvaux, A., Jackson, R., Harman, C.C.D., Li, T., West, A.P., de Zoete, M.R., Wu, Y., Yordy, B., Lakhani, S.A., Kuan, C.Y., et al. (2014). Apoptotic caspases prevent the induction of type I interferons by mitochondrial DNA. Cell *159*, 1563–1577. https://doi.org/10.1016/j.cell.2014.11.037.
39. Eitz Ferrer, P., Potthoff, S., Kirschnek, S., Gasteiger, G., Kastenmüller, W., Ludwig, H., Paschen, S.A., Villunger, A., Sutter, G., Drexler, I., and Häcker, G. (2011). Induction of Noxa-mediated apoptosis by modified vaccinia virus Ankara depends on viral recognition by cytosolic helicases, leading to IRF-3/IFN-β-dependent induction of pro-apoptotic Noxa. PLoS Pathog. *7*, e1002083. https://doi.org/10.1371/journal.ppat.1002083.
40. Gulen, M.F., Koch, U., Haag, S.M., Schuler, F., Apetoh, L., Villunger, A., Radtke, F., and Ablasser, A. (2017). Signalling strength determines proapoptotic functions of STING. Nat. Commun. *8*, e427. https://doi.org/10.1038/s41467-017-00573-w.
41. Corrales, L., Glickman, L.H., McWhirter, S.M., Kanne, D.B., Sivick, K.E., Katibah, G.E., Woo, S.R., Lemmens, E., Banda, T., Leong, J.J., et al. (2015). Direct Activation of STING in the Tumor Microenvironment Leads to Potent and Systemic Tumor Regression and Immunity. Cell Rep. *11*, 1018–1030. https://doi.org/10.1016/j.celrep.2015.04.031.
42. Meric-Bernstam, F., Sweis, R.F., Hodi, F.S., Messersmith, W.A., Andtbacka, R.H.I., Ingham, M., Lewis, N., Chen, X., Pelletier, M., Chen, X., et al. (2022). Phase I Dose-Escalation Trial of MIW815 (ADU-S100), an Intratumoral STING Agonist, in Patients with Advanced/Metastatic Solid Tumors or Lymphomas. Clin. Cancer Res. *28*, 677–688. https://doi.org/10.1158/1078-0432.Ccr-21-1963.
43. Pan, B.S., Perera, S.A., Piesvaux, J.A., Presland, J.P., Schroeder, G.K., Cumming, J.N., Trotter, B.W., Altman, M.D., Buevich, A.V., Cash, B., et al. (2020). An orally available non-nucleotide STING agonist with antitumor activity. Science *369*, eaba6098. https://doi.org/10.1126/science.aba6098.
44. Ramanjulu, J.M., Pesiridis, G.S., Yang, J., Concha, N., Singhaus, R., Zhang, S.Y., Tran, J.L., Moore, P., Lehmann, S., Eberl, H.C., et al. (2018). Design of amidobenzimidazole STING receptor agonists with systemic activity. Nature *564*, 439–443. https://doi.org/10.1038/s41586-018-0705-y.
45. Balka, K.R., Louis, C., Saunders, T.L., Smith, A.M., Calleja, D.J., D'Silva, D.B., Moghaddas, F., Tailler, M., Lawlor, K.E., Zhan, Y., et al. (2020). TBK1 and IKKε Act Redundantly to Mediate STING-Induced NF-κB Responses in Myeloid Cells. Cell Rep. *31*, e107492. https://doi.org/10.1016/j.celrep.2020.03.056.
46. Verzella, D., Pescatore, A., Capece, D., Vecchiotti, D., Ursini, M.V., Franzoso, G., Alesse, E., and Zazzeroni, F. (2020). Life, death, and autophagy in cancer: NF-kappaB turns up everywhere. Cell Death Dis. *11*, e210. https://doi.org/10.1038/s41419-020-2399-y.
47. Bekisz, J., Baron, S., Balinsky, C., Morrow, A., and Zoon, K.C. (2010). Antiproliferative Properties of Type I and Type II Interferon. Pharmaceuticals *3*, 994–1015. https://doi.org/10.3390/ph3040994.
48. Gan, Y., Li, X., Han, S., Liang, Q., Ma, X., Rong, P., Wang, W., and Li, W. (2021). The cGAS/STING Pathway: A Novel Target for Cancer Therapy.

Front. Immunol. *12*, e795401. https://doi.org/10.3389/fimmu.2021.795401.

49. Sejic, N., George, L.C., Tierney, R.J., Chang, C., Kondrashova, O., MacKinnon, R.N., Lan, P., Bell, A.I., Lessene, G., Long, H.M., et al. (2020). BCL-XL inhibition by BH3-mimetic drugs induces apoptosis in models of Epstein-Barr virus-associated T/NK-cell lymphoma. Blood Adv. *4*, 4775–4787. https://doi.org/10.1182/bloodadvances.2020002446.
50. Gram, A.M., Sun, C., Landman, S.L., Oosenbrug, T., Koppejan, H.J., Kwakkenbos, M.J., Hoeben, R.C., Paludan, S.R., and Ressing, M.E. (2017). Human B cells fail to secrete type I interferons upon cytoplasmic DNA exposure. Mol. Immunol. *91*, 225–237. https://doi.org/10.1016/j.molimm.2017.08.025.
51. Amouzegar, A., Chelvanambi, M., Filderman, J.N., Storkus, W.J., and Luke, J.J. (2021). STING Agonists as Cancer Therapeutics. Cancers *13*, e2695. https://doi.org/10.3390/cancers13112695.
52. Harrington, K.J., Brody, J., Ingham, M., Strauss, J., Cemerski, S., Wang, M., Tse, A., Khilnani, A., Marabelle, A., and Golan, T. (2018). Preliminary results of the first-in-human (FIH) study of MK-1454, an agonist of stimulator of interferon genes (STING), as monotherapy or in combination with pembrolizumab (pembro) in patients with advanced solid tumors or lymphomas. Ann. Oncol. *29*, viii712. https://doi.org/10.1093/annonc/mdy424.015.
53. Calvo, E., Garralda, E., Alonso, G., Gambardella, V., Parkes, E.E., Thompson, J., Latek, R., Sikken, P., Schmohl, M., and Harrington, K.J. (2023). 1030P Phase I, first-in-human trial evaluating the STING agonist BI 1387446 alone and in combination with ezabenlimab in solid tumors. Ann. Oncol. *34*, S626. https://doi.org/10.1016/j.annonc.2023.09.2169.
54. Fox, C.P., Civallero, M., Ko, Y.-H., Manni, M., Skrypets, T., Pileri, S., Kim, S.J., Cabrera, M.E., Shustov, A.R., Chiattone, C.S., et al. (2020). Survival outcomes of patients with extranodal natural-killer T-cell lymphoma: a prospective cohort study from the international T-cell Project. Lancet. Haematol. *7*, 284–294. https://doi.org/10.1016/S2352-3026(19)30283-2.
55. Granowicz, E.M., and Jonas, B.A. (2022). Targeting TP53-Mutated Acute Myeloid Leukemia: Research and Clinical Developments. OncoTargets Ther. *15*, 423–436. https://doi.org/10.2147/ott.S265637.
56. Nagata, H., Konno, A., Kimura, N., Zhang, Y., Kimura, M., Demachi, A., Sekine, T., Yamamoto, K., and Shimizu, N. (2001). Characterization of novel natural killer (NK)-cell and gammadelta T-cell lines established from primary lesions of nasal T/NK-cell lymphomas associated with the Epstein-Barr virus. Blood *97*, 708–713. https://doi.org/10.1182/blood.v97.3.708.
57. Coppo, P., Gouilleux-Gruart, V., Huang, Y., Bouhlal, H., Bouamar, H., Bouchet, S., Perrot, C., Vieillard, V., Dartigues, P., Gaulard, P., et al. (2009). STAT3 transcription factor is constitutively activated and is oncogenic in nasal-type NK/T-cell lymphoma. Leukemia *23*, 1667–1678. https://doi.org/10.1038/leu.2009.91.
58. Oyoshi, M.K., Nagata, H., Kimura, N., Zhang, Y., Demachi, A., Hara, T., Kanegane, H., Matsuo, Y., Yamaguchi, T., Morio, T., et al. (2003). Preferential expansion of Vgamma9-JgammaP/Vdelta2-Jdelta3 gamma-delta T cells in nasal T-cell lymphoma and chronic active Epstein-Barr virus infection. Am. J. Pathol. *162*, 1629–1638. https://doi.org/10.1016/s0002-9440(10)64297-6.
59. Chu, V.T., Weber, T., Graf, R., Sommermann, T., Petsch, K., Sack, U., Volchkov, P., Rajewsky, K., and Kühn, R. (2016). Efficient generation of Rosa26 knock-in mice using CRISPR/Cas9 in C57BL/6 zygotes. BMC Biotechnol. *16*, 4–15. https://doi.org/10.1186/s12896-016-0234-4.
60. Koike-Yusa, H., Li, Y., Tan, E.P., Velasco-Herrera, M.D.C., and Yusa, K. (2014). Genome-wide recessive genetic screening in mammalian cells with a lentiviral CRISPR-guide RNA library. Nat. Biotechnol. *32*, 267–273. https://doi.org/10.1038/nbt.2800.
61. Fischer, K.C., Daunt, C.P., Tremblay, C.S., Dias, S., Vince, J.E., and Jabbour, A.M. (2021). Deletion of IKK2 in haematopoietic cells of adult mice leads to elevated interleukin-6, neutrophilia and fatal gastrointestinal inflammation. Cell Death Dis. *12*, e28. https://doi.org/10.1038/s41419-020-03298-9.
62. Schindelin, J., Arganda-Carreras, I., Frise, E., Kaynig, V., Longair, M., Pietzsch, T., Preibisch, S., Rueden, C., Saalfeld, S., Schmid, B., et al. (2012). Fiji: an open-source platform for biological-image analysis. Nat. Methods *9*, 676–682. https://doi.org/10.1038/nmeth.2019.
63. Kroon, E., Krosl, J., Thorsteinsdottir, U., Baban, S., Buchberg, A.M., and Sauvageau, G. (1998). Hoxa9 transforms primary bone marrow cells through specific collaboration with Meis1a but not Pbx1b. EMBO J. *17*, 3714–3725. https://doi.org/10.1093/emboj/17.13.3714.
64. Aubrey, B.J., Kelly, G.L., Kueh, A.J., Brennan, M.S., O'Connor, L., Milla, L., Wilcox, S., Tai, L., Strasser, A., and Herold, M.J. (2015). An inducible lentiviral guide RNA platform enables the identification of tumor-essential genes and tumor-promoting mutations in vivo. Cell Rep. *10*, 1422–1432. https://doi.org/10.1016/j.celrep.2015.02.002.
65. La Marca, J.E., Aubrey, B.J., Yang, B., Chang, C., Wang, Z., Kueh, A., Tai, L., Wilcox, S., Milla, L., Heinzel, S., et al. (2024). Genome-wide CRISPR screening identifies a role for ARRDC3 in TRP53-mediated responses. Cell Death Differ. *31*, 150–158. https://doi.org/10.1038/s41418-023-01249-3.
66. Bronner, D.N., and O'Riordan, M.X. (2016). Measurement of Mitochondrial DNA Release in Response to ER Stress. Bio. Protoc. *6*, e1839. https://doi.org/10.21769/BioProtoc.1839.
67. Bryant, J.D., Lei, Y., VanPortfliet, J.J., Winters, A.D., and West, A.P. (2022). Assessing Mitochondrial DNA Release into the Cytosol and Subsequent Activation of Innate Immune-related Pathways in Mammalian Cells. Curr. Protoc. *2*, e372. https://doi.org/10.1002/cpz1.372.
68. Barretina, J., Caponigro, G., Stransky, N., Venkatesan, K., Margolin, A.A., Kim, S., Wilson, C.J., Lehár, J., Kryukov, G.V., Sonkin, D., et al. (2012). The Cancer Cell Line Encyclopedia enables predictive modelling of anticancer drug sensitivity. Nature *483*, 603–607. https://doi.org/10.1038/nature11003.
69. Bairoch, A. (2018). The Cellosaurus, a Cell-Line Knowledge Resource. J. Biomol. Tech. *29*, 25–38. https://doi.org/10.7171/jbt.18-2902-002.
70. Wickham, H. (2016). ggplot2: Elegant Graphics for Data Analysis (Springer-Verlag). https://doi.org/10.1007/978-3-319-24277-4.
71. Galaxy Community (2022). The Galaxy platform for accessible, reproducible and collaborative biomedical analyses: 2022 update. Nucleic Acids Res. *50*, W345–W351. https://doi.org/10.1093/nar/gkac247.
72. Kim, D., Langmead, B., and Salzberg, S.L. (2015). HISAT: a fast spliced aligner with low memory requirements. Nat. Methods *12*, 357–360. https://doi.org/10.1038/nmeth.3317.
73. Liao, Y., Smyth, G.K., and Shi, W. (2014). featureCounts: an efficient general purpose program for assigning sequence reads to genomic features. Bioinformatics *30*, 923–930. https://doi.org/10.1093/bioinformatics/btt656.
74. Law, C.W., Chen, Y., Shi, W., and Smyth, G.K. (2014). voom: Precision weights unlock linear model analysis tools for RNA-seq read counts. Genome Biol. *15*, R29. https://doi.org/10.1186/gb-2014-15-2-r29.
75. Robinson, M.D., and Oshlack, A. (2010). A scaling normalization method for differential expression analysis of RNA-seq data. Genome Biol. *11*, R25. https://doi.org/10.1186/gb-2010-11-3-r25.
76. Benjamini, Y., and Hochberg, Y. (1995). Controlling the false discovery rate: a practical and pwerful approach to multiple testing. J. R. Stat. Soc. Series B Methodol. *57*, 289–300. https://doi.org/10.1111/j.2517-6161.1995.tb02031.x.
77. Liberzon, A., Birger, C., Thorvaldsdóttir, H., Ghandi, M., Mesirov, J.P., and Tamayo, P. (2015). The Molecular Signatures Database Hallmark Gene Set Collection. Cell Syst. *1*, 417–425. https://doi.org/10.1016/j.cels.2015.12.004.
78. Liberzon, A., Subramanian, A., Pinchback, R., Thorvaldsdóttir, H., Tamayo, P., and Mesirov, J.P. (2011). Molecular signatures database (MSigDB) 3.0. Bioinformatics *27*, 1739–1740. https://doi.org/10.1093/bioinformatics/btr260.
79. Garnham, A. (2020). Mouse and Human Versions of the MSigDB in R Format. https://bioinf.wehi.edu.au/MSigDB/index.html.
80. Korotkevich, G., Sukhov, V., Budin, N., Shpak, B., Artyomov, M.N., and Sergushichev, A. (2021). Fast gene set enrichment analysis. Preprint at bioRxiv *1*. https://doi.org/10.1101/060012.

Please cite this article in press as: Diepstraten et al., Putting the STING back into BH3-mimetic drugs for *TP53*-mutant blood cancers, Cancer Cell (2024), https://doi.org/10.1016/j.ccell.2024.04.004

STAR★METHODS

KEY RESOURCES TABLE

REAGENT or RESOURCE	SOURCE	IDENTIFIER
Antibodies		
CD45-FITC (1:100)	Beckman Coulter	Cat# IM0782U; RRID: AB_131000
CD34-PerCP-Cy5 (1:25)	BD Biosciences	Cat# 347203; RRID: AB_400266
CD117-PE-Cy7 (1:100)	BioLegend	Cat# 313212; RRID: AB_893222
HLA-DR-APC-Cy7 (1:50)	Abcam	Cat# ab239308
CD33-BV650 (1:100)	BioLegend	Cat# 303430; RRID: AB_2650933
CD33-APC (1:100)	BioLegend	Cat# 983902; RRID: AB_2810824
CD14-Alexa Fluor 700 (1:100)	BioLegend	Cat# 367114; RRID: AB_2566716
CD64-BV786 (1:50)	BioLegend	Cat# 305044; RRID: AB_2800780
CD3-BV421 (1:100)	BD Horizon	Cat# 562426; RRID: AB_11152082
CD3-B711 (1:100)	BD Horizon	Cat# 563725; RRID: AB_2744392
CD19-PE (1:100)	Beckman Coulter	Cat# IM1285U; RRID: AB_10640419
CD16-BV650 (1:50)	BioLegend	Cat# 302042; RRID: AB_11125578
CD56-BV650 (1:50)	BioLegend	Cat# 362532; RRID: AB_2565602
B220-BV605 (1:200)	BioLegend	Cat# 103244; RRID: AB_2563312
CD19-APC (1:400)	WEHI Antibody Facility	1D3
IgM-FITC (1:400)	WEHI Antibody Facility	5–1
IgD-PE (1:800)	BD Pharmingen	Cat# 558597; RRID: AB_647211
cKit-BV711 (1:200)	BD Horizon	Cat# 563160; RRID: AB_2722510
Anti-FCR (1:10)	made in-house	N/A
TCRβ-PeCy7 (1:400)	BioLegend	Cat# 109222; RRID: AB_893627
CD4-PerCP (1:800)	BioLegend	Cat# 100434; RRID: AB_893330
CD8-Alexa Fluor 700 (1:400)	WEHI Antibody Facility	53-6-7
TER119-Alexa Fluor 647 (1:400)	WEHI Antibody Facility	TER119
Mac1- APC-Cy7 (1:400)	BD Pharmingen	Cat# 557657; RRID: AB_396772
Gr-1-PE (1:400)	WEHI Antibody Facility	RB6-8C5
NK1.1-Alexa Fluor 700 (1:400)	WEHI Antibody Facility	6-3-17
CD11c- FITC (1:400)	WEHI Antibody Facility	N418
mCD45-BV711	BD Biosciences	Cat# 564357; RRID: AB_2744404
HSP70 (reactivity: mouse/human, host species: mouse, dilution: 1:10000)	Dr. R. Anderson (ONJCRI, Australia)	Clone: N6
TRP53 (reactivity: mouse, host species: rabbit, dilution: 1:2000)	Novocastra	Cat# NCL-p53-CM5p; RRID: AB_563933; Clone: CM5
TP53 (reactivity: human, host species: mouse, dilution: 1:1000)	Santa Cruz Biotechnology	Cat# sc-126; RRID: AB_628082; Clone: DO-1
PUMA (reactivity: mouse/human, host species: rabbit, dilution: 1:500)	ProSci Incorporated	Cat# 3043; RRID: AB_203251; Clone: polyclonal
BIM (reactivity: mouse/human, host species: rabbit, dilution: 1:1000)	Enzo Life Sciences	Cat# ADI-AAP-330-E; RRID: AB_2038875; Clone: polyclonal
STING (reactivity: mouse/human, host species: rabbit, dilution: 1:1000)	Cell Signaling Technology	Cat# 13647; RRID: AB_2732796; Clone: D2P2F
pSTING (reactivity: mouse, host species: rabbit, dilution: 1:1000)	Cell Signaling Technology	Cat# 72971; RRID: AB_2799831; Clone: D8F4W
pSTING (reactivity: human, host species: rabbit, dilution: 1:1000)	Cell Signaling Technology	Cat# 19781; RRID: AB_2737062; Clone: D7C3S

(*Continued on next page*)

Continued

REAGENT or RESOURCE	SOURCE	IDENTIFIER
TBK1 (reactivity: mouse/human, host species: rabbit, dilution: 1:1000)	Cell Signaling Technology	Cat# 3504; RRID: AB_2255663; Clone: D1B4
pTBK1 (reactivity: mouse/human, host species: rabbit, dilution: 1:1000)	Cell Signaling Technology	Cat# 5483; RRID: AB_10693472; Clone: D52C2
IRF3 (reactivity: mouse/human, host species: rabbit, dilution: 1:1000)	Cell Signaling Technology	Cat# 4302; RRID: AB_1904036; Clone: D83B9
pIRF3 (reactivity: mouse/human, host species: rabbit, dilution: 1:1000)	Cell Signaling Technology	Cat# 4947; RRID: AB_823547; Clone: 4D4G
BCL-2 (reactivity: mouse/human, host species: mouse, dilution: 1:2000)	BD Biosciences	Cat# 610539; RRID: AB_397896; Clone: 7/BCL-2
cGAS (reactivity: mouse, host species: rabbit, dilution: 1:1000)	Cell Signaling Technology	Cat# 31659; RRID: AB_2799008; Clone: D3O8O
Mouse IgG (host species: goat, dilution: 1:2000)	Southern Biotech	Cat# 1010-05; RRID: AB_2728714
Rabbit IgG (host species: goat, dilution: 1:5000)	Southern Biotech	Cat# 4010-05; RRID: AB_2632593
Biological samples		
Human AML: PDX 1: genotyping information in Table S1	this paper	PDX-32
Human AML: PDX 2: genotyping information in Table S1	this paper	PDX-20
Human AML: 03-271-2022: genotyping information in Table S1	this paper	N/A
Human AML: 01-335-2022: genotyping information in Table S1	this paper	N/A
Human AML: 02-104-2023: genotyping information in Table S1	this paper	N/A
Human AML: 01-117-2023: genotyping information in Table S1	this paper	N/A
Human AML: 05-016-2023: genotyping information in Table S1	this paper	N/A
Human AML: 01-021-2019: genotyping information in Table S1	this paper	N/A
Human AML: 01-058-2023: genotyping information in Table S1	this paper	N/A
Chemicals, peptides, and recombinant proteins		
S63845	Chemgood	Cat# C1370
diABZI Sting agonist 3	SYNthesis Med Chem	N/A
A-1331852	Dr N Duong and Prof G Lessene (WEHI, Australia)	N/A
ABT-199/venetoclax	Active Biochem	Cat# A-1231
ADU-S100	MedChemExpress	Cat# HY-12885A
MSA-2	MedChemExpress	Cat# HY-136927
TPCA-1	MedChemExpress	Cat# HY-10074
GSK8612	MedChemExpress	Cat# HY-111941
doxorubicin	Ebewe Interpharma	N/A
ionomycin	Sigma-Aldrich	Cat# I9657
nutlin-3a	MedChemExpress	Cat# HY-10029
thapsigargin	Sigma-Aldrich	Cat# T9033
QVD-O-Ph	MedChemExpress	Cat# HY-12305
hIL-3	R&D Systems	Cat# 203-IL
hIL-6	R&D Systems	Cat# 206-IL
hFLT3-ligand	R&D Systems	Cat# 308-KFN

(*Continued on next page*)

Continued

REAGENT or RESOURCE	SOURCE	IDENTIFIER
hSCF	R&D Systems	Cat# 255-SC
mIL-3	In house	N/A
hIL-2	PeproTech	Cat #200-02
Critical commercial assays		
MycoAlert	Lonza	Cat #LT07
eBioscience Foxp3/Transcript Factor Staining Buffer Set	Invitrogen	Cat# 00-5523-00
SF Cell Line 4D-Nucleofector X Kit	Lonza	Cat# V4XC-2023
DNeasy Blood & Tissue Kit	QIAGEN	Cat# 69504
GoTaq Green Master Mix	Promega	Cat# M712
Pierce BCA Protein Assay Kit	Thermo Fisher Scientific	Cat# 23225
TaqMan Fast Advanced Master Mix	Thermo Fisher Scientific	Cat# 4444963
Superscript III First Strand Synthesis System	Thermo Fisher Scientific	Cat# 18080051
TruSeq RNA Library Prep Kit v2	Illumina	Cat# RS-122-2001
SYBR Green PCR Master Mix	Thermo Fisher Scientific	Cat# 4309155
Deposited data		
Eμ-Myc RNA-seq data	this paper	GEO: GSE261373
Mouse reference genome GRCm38 (mm10)	Genome Reference Consortium	https://www.ncbi.nlm.nih.gov/datasets/genome/GCF_000001635.20/
MSigDB Hallmark collection (mapped to mouse orthologues)	Garnham 2020[79]	https://bioinf.wehi.edu.au/MSigDB/index.html
Experimental models: Cell lines		
Murine B cell lymphoma: AH15A: *Eμ-Myc*	Kotschy et al. 2016[32]	N/A
Murine B cell lymphoma: AF47A: *Eμ-Myc*	Kotschy et al. 2016[32]	N/A
Murine B cell lymphoma: 560: *Eμ-Myc*	Kotschy et al. 2016[32]	N/A
Murine double-hit lymphoma: 214DHL: *Eμ-Myc/dCas9a-SAM+/−/sgBcl-2*	Deng et al. 2022[33]	N/A
Murine double-hit lymphoma: 216DHL: *Eμ-Myc/dCas9a-SAM+/−/sgBcl-2*	Deng et al. 2022[33]	N/A
Murine double-hit lymphoma: 270DHL: *Eμ-Myc/dCas9a-SAM+/−/sgBcl-2*	Deng et al. 2022[33]	N/A
Human Burkitt lymphoma: BL2	Dr A Rickinson (The University of Birmingham, UK)	RRID: CVCL_1966
Human Burkitt lymphoma: Akata-BL	Prof K Takada (Hokkaido University, Japan)	RRID: CVCL_0148
Human Burkitt lymphoma: Ramos-BL	Dr S Cory (WEHI, Australia)	RRID: CVCL_0597
Human DLBCL: DOHH2	Dr D Huang (WEHI, Australia)	RRID: CVCL_1179
Human AML: MV4; 11	Dr D Huang (WEHI, Australia)	RRID: CVCL_0064
Human AML: THP-1	Dr D Huang (WEHI, Australia)	RRID: CVCL_0006
Human AML: MOLM-13	Dr D Huang (WEHI, Australia)	RRID: CVCL_2119
Human AML: KASUMI-1	Dr D Huang (WEHI, Australia)	RRID: CVCL_0589
Human AML: HL-60	Dr D Huang (WEHI, Australia)	RRID: CVCL_0002
Human AML: KG-1	Dr D Huang (WEHI, Australia)	RRID: CVCL_0374
Human AML: OCI-AML-3	Dr D Huang (WEHI, Australia)	RRID: CVCL_1844
Human ENKT: SNK6	Dr C Shannon-Lowe (The University of Birmingham, UK), Nagata et al. 2001[56]	RRID: CVCL_A673
Human ENKT: MEC04:	Dr C Shannon-Lowe (The University of Birmingham, UK), Coppo et al. 2009[57]	N/A
Human ENKT: SNT15	Dr C Shannon-Lowe (The University of Birmingham, UK), Oyoshi et al. 2003[58]	RRID: CVCL_A675

(*Continued on next page*)

Please cite this article in press as: Diepstraten et al., Putting the STING back into BH3-mimetic drugs for *TP53*-mutant blood cancers, Cancer Cell (2024), https://doi.org/10.1016/j.ccell.2024.04.004

Continued

REAGENT or RESOURCE	SOURCE	IDENTIFIER
Human ENKT: SNT8	Dr C Shannon-Lowe (The University of Birmingham, UK), Nagata et al. 2001[56]	RRID: CVCL_A677
Human ENKT: NKCI	Dr C Shannon-Lowe (The University of Birmingham, UK)	N/A
Human embryonic kidney: HEK293T	ATCC	RRID: CVCL_0063; Cat #CRL216
Murine AML: 556: *HoxA9/Meis1*	this paper	N/A
Murine AML: 557: *HoxA9/Meis1*	this paper	N/A
Murine AML: 558: *HoxA9/Meis1*	this paper	N/A
Murine AML: 559: *HoxA9/Meis1*	this paper	N/A
Murine AML: 561: *HoxA9/Meis1*	this paper	N/A
Experimental models: Organisms/strains		
Mouse: *Rag1*$^{-/-}$: *C57BL/6-WEHI Rag1*$^{-/-}$	WEHI breeding facility	N/A
Mouse: *C57BL/6 Cas9*$^{KI/KI}$: *C57BL/6-WEHI Cas9*$^{KI/KI}$	Prof K.Rajewsky (Max Delbrück Center, Germany), Chu et al. 2016[59]	RRID: IMSR_JAX:02855
Mouse: *NSG*: *NOD-SCID-*$\gamma_c{}^{-/-}$	WEHI breeding facility	N/A
Mouse: NSG-SG3: *NOD.Cg-Prkdc*^{scid} *Il2rg*^{tm1Wjl} *Tg(CMV-IL3,CSF2,KITLG)1 Eav/MloySzJ*	The Jackson Laboratory	RRID: IMSR_JAX:013062
Mouse: C57BL/6: *C57BL/6-WEHI*	WEHI breeding facility	N/A
Oligonucleotides		
sgRNAs can be found in Table S2	this paper	N/A
Primers for NGS can be found in Table S3	this paper	N/A
Primers for mtDNA quantification can be found in Table S3	Bronner et al. 2016[66]; Bryant et al. 2022[67]	N/A
Recombinant DNA		
FuCas9-Cherry	Addgene, Aubrey et al. 2015[64]	Cat #70182
FgH1tUTG	Addgene, Aubrey et al. 2015[64]	Cat #70183
pKLV-U6gRNA(Bbsl)-PGKpuro2ABFP	Addgene, Koike-Yusa et al. 2014[60]	Cat #50946
Software and algorithms		
Prism v9	GraphPad	
FlowJo v10	BD Biosciences	
ImageJ/Fiji	Schindelin et al. 2012[62]	
CRISPR indel calculator	Dr ST Diepstraten	https://crisprindelcalc.net
Galaxy Australia	The Galaxy Community 2022[71]	https://usegalaxy.org.au/
HISAT2 v2.2.1	Kim et al. 2015[72]	via Galaxy Australia (https://usegalaxy.org.au/)
subread v2.0.3	Liao et al. 2014[73]	via Galaxy Australia (https://usegalaxy.org.au/)
limma-voom v3.50.1	Law et al. 2014[74]	via Galaxy Australia (https://usegalaxy.org.au/)
ggplot2 v3.3.3	Wickham et al. 2016[70]	via Galaxy Australia (https://usegalaxy.org.au/)
fgsea v1.8.0	Korotkevich et al. 2021[80]	via Galaxy Australia (https://usegalaxy.org.au/)
Other		
Zombie Yellow (1:1000)	BioLegend	Cat# 423103
LIVE/DEAD Fixable Yellow	Invitrogen	Cat# L34959
AmPure XP beads	Beckman Coulter	Cat# A63880
TRIzol	Thermo Fisher Scientific	Cat# 15596026
Taqman probe (mouse): *Hmbs*	Thermo Fisher Scientific	Mm01143545_m1
Taqman probe (mouse): *Noxa/Pmaip1*	Thermo Fisher Scientific	Mm00451763_m1
Taqman probe (mouse): *Puma/Bbc3*	Thermo Fisher Scientific	Mm00519268_m1
Taqman probe (mouse): *Bim/Bcl2l11*	Thermo Fisher Scientific	Mm00437796_m1
Taqman probe (mouse): *Trp53*	Thermo Fisher Scientific	Mm01731287_m1

(*Continued on next page*)

Continued

REAGENT or RESOURCE	SOURCE	IDENTIFIER
Taqman probe (mouse): *Irf7*	Thermo Fisher Scientific	Mm00516793_g1
Taqman probe (mouse): *p21/Cdkn1a*	Thermo Fisher Scientific	Mm00432448_m1
Taqman probe (mouse): *Ifnb1*	Thermo Fisher Scientific	Mm00439552_s1
Taqman probe (mouse): *Cxcl10*	Thermo Fisher Scientific	Mm00445235_m1
Taqman probe (mouse): *Il6*	Thermo Fisher Scientific	Mm00446190_m1
Taqman probe (mouse): *Ifit1*	Thermo Fisher Scientific	Mm00515153_m1
Taqman probe (human): *HMBS*	Thermo Fisher Scientific	Hs00609296_g1
Taqman probe (human): *NOXA/PMAIP1*	Thermo Fisher Scientific	Hs00560402_m1
Taqman probe (human): *BIM/BCL2L11*	Thermo Fisher Scientific	Hs00708019_s1
Taqman probe (human): *PUMA/BBC3*	Thermo Fisher Scientific	Hs00248075_m1
Taqman probe (human): *P21/CDKN1A*	Thermo Fisher Scientific	Hs00355782_m1
Taqman probe (human): *IFNB1*	Thermo Fisher Scientific	Hs01077958_s1
Taqman probe (human): *GAPDH*	Thermo Fisher Scientific	Hs02786624_g1

RESOURCE AVAILABILITY

Lead contact

Further information and requests for resources and reagents should be directed to and will be fulfilled by the lead contact, A/Prof Gemma Kelly (gkelly@wehi.edu.au).

Materials availability

This study did not generate new unique reagents.

Data and code availability

- RNA-seq data have been deposited at GEO and are publicly available as of the date of publication. Accession numbers are listed in the key resources table.
- This paper does not report original code.
- Any additional information required to reanalyze the data reported in this paper is available from the lead contact upon request.

EXPERIMENTAL MODEL AND STUDY PARTICIPANT DETAILS

Cancer cell lines and tissue culture

Mouse *Eμ-Myc* lymphoma cell lines AH15A, AF47A and 560 were previously derived from tumors arising in *Eμ-Myc* mice (C57BL/6-WEHI)[32] and cultured in FMA medium consisting of high glucose DMEM supplemented with 10% heat-inactivated fetal bovine serum (FBS; Sigma #F9423), 100 μM L-asparagine (Sigma #A4284), 50 μM β-mercaptoethanol (Sigma #M3148), 100 U/mL penicillin and 100 mg/mL streptomycin (Gibco #15140122). Mouse cells were maintained at 37°C with 10% CO_2. Mouse double hit lymphoma cell lines 214DHL, 216DHL and 270DHL were derived from tumors arising in *Eμ-Myc/dCas9a-SAM*$^{+/-}$*/sgBcl-2* mice as described previously[33] and cultured as above. The human Burkitt lymphoma cell lines BL2 (a kind gift from Dr A Rickinson, The University of Birmingham, UK) and Akata-BL (a kind gift from Prof K Takada, Hokkaido University, Japan), were cultured in RPMI-1640 medium supplemented with 10% FBS, 1 mM sodium pyruvate (Gibco #11360070), 2 mM L-glutamine (Gibco #25030081), 50 μM α-thioglycerol (Sigma #M-6145), 100 U/mL penicillin and 100 μg/mL streptomycin. The human DLBCL cell line DOHH2 (a kind gift from Prof D Huang, The Walter and Eliza Hall Institute, Australia), Burkitt lymphoma cell line Ramos-BL (a kind gift from Prof S Cory, The Walter and Eliza Hall Institute, Australia) and all AML cell lines (MV4; 11, MOLM-13, THP-1, KASUMI-1, HL-60, KG1 and OCI-AML3; a kind gift from Prof D Huang) were cultured in RPMI-1640 medium supplemented with 10% heat-inactivated FBS, 100 U/mL penicillin and 100 μg/mL streptomycin. The human ENKT lymphoma cell lines SNK6,[56] MEC04,[57] SNT15,[58] NKCI and SNT8[56] (a kind gift from Dr C Shannon-Lowe, The University of Birmingham, UK) were cultured in RPMI-1640 medium supplemented with 10% heat-inactivated human serum (Sigma #H4552), 1 mM sodium pyruvate, 2 mM L-glutamine, 700 U/mL human IL-2 (PeproTech #200-02), 100 U/mL penicillin and 100 μg/mL streptomycin. Human lymphoma and leukemia cell lines were maintained at 37°C with 5% CO_2 and verified by STR profiling at the Australian Genomics Research Facility (AGRF). Human cell lines of both male and female origin were included in the study. HEK293T (ATCC #CRL-3216) cells were cultured in DMEM supplemented with 10% FBS, 100 U/mL penicillin and 100 mg/mL streptomycin and maintained at 37°C with 10% CO_2. All cell lines were passaged in culture for <3 months and regularly tested negative for mycoplasma (MycoAlert; Lonza #LT07).

Primary AML and healthy donor specimens

Bone marrow and peripheral blood samples were collected from patients treated at The Peter MacCallum Cancer Center and The Alfred Hospital who had newly diagnosed or morphologically relapsed AML. Peripheral blood samples from healthy donors (equal numbers male and female) were collected at the Walter and Eliza Hall Institute of Medical Research. Samples were collected after informed consent and studies were conducted in accordance with the approved protocols through the Human Research Ethics Committee of the respective institutions and the Declaration of Helsinki. Mononuclear cells were isolated using Ficoll density gradient. Freshly processed or thawed cryopreserved cells were used in drug sensitivity assays. Cells were cultured in Stempsan SFEM (Stem Cell Technologies #09650), supplemented with Stemreginin (500 nM; StemCell Technologies #72354), UM171 (35 nM; Selleckchem #S7608), and recombinant human cytokines IL-3 (1 ng/mL; R&D Systems #203-IL), IL-6 (2 ng/mL; R&D Systems #206-IL), FLT3-ligand (5 ng/mL; R&D Systems #308-KFN) and stem cell factor (5 ng/mL; R&D Systems #255-SC).

Mice

All experiments with animals followed the guidelines of the Melbourne Directorate Animal Ethics Committee and were approved by The Walter and Eliza Hall Institute of Medical Research Ethics Committee. Mice were group-housed (up to 6 per cage) and maintained on Barastoc rodent diet (Barastoc #102093). For experiments, littermates were randomly assigned to treatment arms. Individual experiments were performed with cohorts of either all female or all male mice as indicated in the method details. Mice were excluded from analyses if they were euthanised for unrelated illnesses and did not complete treatment (as described in Figure 5F and S7).

METHOD DETAILS

Eμ-Myc lymphoma mouse experiments

For *in vivo* experiments with *Eμ-Myc* lymphoma cells, healthy *Rag1*$^{-/-}$ (male, 6–10 weeks old) or *C57BL/6 Cas9*$^{KI/KI}$ (male, 11–30 weeks old) mice[59] were intravenously (IV) injected with 1 × 10^6 AH15A wild-type or *Trp53* KO cells on day 0. On days 4–8 post-transplantation, mice were treated with 25 mg/kg S63845 (Chemgood #C1370) or vehicle (50 mM PBS containing 2% vitamin E (Sigma #57668)) daily by IV injection. On days 4, 7 and 11 post-transplantation, mice were treated with 1.5 mg/kg diABZI Sting agonist compound 3 (diABZI; SYNthesis Med Chem) or vehicle (40% polyethylene glycol(PEG)-400 (Sigma #P3265) in saline) by IV injection (n = 4–6 per treatment arm). On days where both drugs were administered, diABZI was given 4 h after S63845 to allow mice to recover from handling. Mice were monitored for lymphoma by experienced animal technicians who were blinded to the nature of the transplanted tumor cells and the treatments applied, and animals were euthanized at the predetermined ethical endpoint. Experiments concluded 150 days post-transplant and any remaining (lymphoma free) mice were euthanized. For all mice, retro-orbital bleeds were analyzed by Advia to obtain blood cell counts, and enlarged organs (spleen, lymph nodes, thymus) were weighed.

Human ENKT lymphoma xenograft experiments

For *in vivo* ENKT lymphoma xenograft experiments, healthy *NOD-SCID-*$\gamma_c^{-/-}$ (*NSG*) mice (male, 6–8 weeks old) were subcutaneously injected with 2 × 10^6 SNK6 human ENKT lymphoma cells on day 0. On days 7–13 post-transplantation, mice were treated by oral gavage with 50 mg/kg of the BCl-XL inhibitor A-1331852 (a kind gift from Dr D Nhu and Prof G Lessene, WEHI) or vehicle (2.5% DMSO, 10% EtOH, 27.5% PEG-400, 60% Phosal 50 PG (Lipoid/Thermo Fisher Scientific #FSHNC0130871)). On days 7, 10 and 13 post-transplantation, mice were treated with 1.5 mg/kg diABZI or vehicle (40% PEG-400 in 0.9% saline) by IV injection (n = 6 per treatment arm). On days where both drugs were administered, diABZI was given 4 h after A-1331852 to allow mice to recover from handling. Mice were checked for tumors by experienced animal technicians, who were blinded to the treatments applied, 3 times weekly by thorough examination and probing of the injection site. Once detected, tumors were measured using calipers every 3–4 days by an experienced animal technician who was blinded to the treatment applied. Tumor volume was calculated using the equation $\pi/6 \times \text{length} \times \text{width}^2$. Mice were euthanized at ethical endpoint when tumors had reached 0.5 cm^3. The volumes of tumors in mice treated with A-1331852, or A-1331852 in combination with diABZI, which arose later than those in the vehicle or diABZI only treatment arms, could not be accurately measured using calipers, due to their varying shapes/positions. Therefore, these mice were collected on day 65 post-transplantation, tumors excised from the right flank and tumor weights compared directly. For all mice, retro-orbital bleeds were analyzed by Advia to obtain blood cell counts, and spleens, enlarged lymph nodes and tumors were weighed.

Human AML xenograft mouse experiments

For *in vivo* studies, venetoclax was dissolved in 60% Phosal 50 PG, 30% PEG-400 (Sigma #202398) and 10% EtOH. For AML cell line xenograft experiments, healthy *NSG* mice (female, 8–10 weeks old) were injected with 2.5 × 10^5 MOLM-13 *TP53*-wild-type or *TP53* KO cells intravenously on day 0. From day 3, mice received either no treatment (control), venetoclax (50 mg/kg orally 5× weekly), diABZI (1.5 mg/kg intravenously 2× weekly), or the drug combination for two weeks (n = 5 per treatment arm). On days where both drugs were administered, they were administered simultaneously. For AML patient derived xenograft (PDX) experiments, healthy *NSG-SG3* (female, 8 weeks old) mice were intravenously injected with 5 × 10^5 cryopreserved patient AML samples. Human leukemia engraftment was confirmed using flow cytometric analysis of submandibular peripheral blood for the presence of hCD45+ cells (any %; hCD45-FITC 1:100; Beckman Coulter #IM0782U; mCD45-BV711 1:1000; BD Biosciences #564357). For PDX model #1, confirmation of engraftment was obtained on day 21 post-transplant and treatment commenced on day 25. For PDX model #2,

confirmation of engraftment was obtained on day 21 post-transplant and treatment commenced on day 24. Mice were left untreated or administered with venetoclax (50 mg/kg orally 5× weekly), diABZI (1.5 mg/kg intravenously 2× weekly), or the drug combination for four weeks (n = 6 per treatment arm). Leukemia progression was monitored using intrafemoral biopsy during week 2 of therapy. Briefly, mice were anesthetized with isofluorane and administered with analgesics 0.1 mg/kg buprenorphine and 5 mg/kg carprofen. Femoral bone marrow was aspirated using a 27-gauge syringe and needle and percentage hCD45+ leukemia cells was enumerated by flow cytometry. Mice were monitored for leukemia development and euthanized at predetermined ethical endpoint. Drug efficacy was determined by flow cytometric assessment of peripheral blood, bone marrow, and spleens (if enlarged) to assess leukemia burden (by hCD33+ (CD33-APC) for cell line xenografts and hCD45+ (CD45-FITC) for PDXs). Viability was assessed by LIVE/DEAD Fixable Yellow (Invitrogen #L34959) and cells were fixed with eBioscience Foxp3/Transcript Factor Staining Buffer Set (Invitrogen #00-5523-00) before analysis on an Aurora flow cytometer (Cytek).

Drug toxicity experiments in mice

To measure acute drug toxicity *in vivo*, healthy C57BL/6-WEHI mice (male, 6–8 week old) were treated with vehicle (for S63845; IV), S63845 (25 mg/kg; IV), vehicle (for venetoclax; oral gavage) or venetoclax (50 mg/kg; oral gavage). After 4 h, mice were treated with vehicle (for diABZI; IV) or diABZI (1.5 mg/kg; IV). 24 h after the initial BH3-mimetic treatment, a retro-orbital bleed was taken for analysis by Advia. Graphs were prepared in Prism v9 (GraphPad).

To measure long term recovery, C56BL/6-WEHI mice were treated with dosing schedules matching that used in AML experiments for two weeks (5× weekly venetoclax, 50 mg/kg oral gavage and/or 2× weekly diABZI, 1.5 mg/kg IV). Body weight was monitored every 2–3 days. The mice were collected 96 h following the final treatment. Retro-orbital bleeds and bone marrow from the femur and tibia were collected for analysis of immune cell populations by flow cytometry. Briefly, red cells were lysed and live cells were stained with Zombie Yellow (BioLegend #423103) for 15 min on ice. Cells were then stained on ice for 1 h with extracellular markers for lineage identification (key resources table). Cells were then fixed with 4% PFA for 1 h on ice. Samples were analyzed on an Aurora flow cytometer (Cytek). Data were plotted in Prism v9.

CRISPR-Cas9 gene knockout cell lines

CRISPR-Cas9 gene editing for mouse and human lymphoma cell lines was performed using FuCas9-Cherry (Addgene Plasmid #70182) and FgH1tUTG (Addgene Plasmid #70183) lentiviral constructs as described previously.[20] Parental cells expressing *Cas9* and a non-targeting (NT) control sgRNA against human *BIM* (for mouse cell lines) or mouse *Bim* (for human cell lines) were used as control (NTC) cells for all experiments involving CRISPR-Cas9 generated cell lines. Successful knockout of targeted proteins was confirmed by immunoblotting or next generation sequencing. For AML cell lines, sgRNA guides targeting human *TP53*, *STING*, *BAX*, *BAK* and non-targeting control guides were obtained from the Sanger Whole Genome CRISPR Arrayed Library or synthesized (Integrated DNA Technologies) and cloned into pKLV-U6gRNA(Bbsl)-PGKpuro2ABFP (Addgene Plasmid #50946[60]) or FgH1tUTG (Addgene Plasmid #70183). *TP53* and *STING* double KO cells were generated by electroporation of *STING* sgRNAs (purchased from Synthego) into *TP53* KO cells using the SF Cell Line 4D-Nucleofector X Kit (Lonza #V4XC-2023) and 4D-Nucleofector Core Unit (Lonza). The sgRNA sequences used are listed in Table S2.

Next generation sequencing

Next generation sequencing was performed to confirm successful CRISPR-Cas9-mediated gene mutation. For mouse *Eμ-Myc* lymphomas and human B cell lymphomas, genomic DNA was extracted using the DNeasy Blood & Tissue Kit (QIAGEN #69504). sgRNA target sites were PCR-amplified using GoTaq green mix (Promega #M712) and gene-specific primers with overhangs to enable indexing of products and sequencing on the Illumina platform. Primer sequences are listed in Table S3. The following cycling conditions were used: denaturation at 95°C for 3 min, followed by 35 cycles of 95°C for 30 s, 60°C for 30 s and 72°C for 30 s. The final extension was performed at 72°C for 5 min. Samples were pooled and cleaned up using AmPure XP beads (Beckman Coulter #A63880) and sequenced on an Illumina MiSeq. For human AMLs, sequencing for *TP53* mutations was performed as described previously using published primer sequences.[26] The proportion of indels was determined using the CRISPR indel calculator https://crisprindelcalc.net and graphs generated in Prism v9.

Cell line death assays

Cells were plated into 96-well flat-bottom plates in duplicate at 3×10^4 cells/well and drugs added at indicated concentrations. The following drugs were used: S63845, A-1331852, ABT-199/venetoclax (Active Biochem #A-1231), ADU-S100 (MedChemExpress #HY-12885A), MSA-2 (MedChemExpress #HY-136927), TPCA-1 (MedChemExpress #HY-10074), GSK8612 (MedChemExpress #HY-111941), diABZI, doxorubicin (Ebewe Interpharma), and ionomycin (Sigma-Aldrich #I9657). All drugs were dissolved in DMSO except for ADU-S100 which was dissolved in H_2O. At the indicated time point, cells were transferred into a round-bottom 96-well plate, spun down at 1500 rpm for 5 min, resuspended in Annexin V binding buffer containing Annexin V-A647 (made in house, 1:2000) and propidium iodide (PI; 1 μg/mL). Live cells (Annexin V/PI double-negative) were quantified on an LSR II flow cytometer (BD Biosciences). For the human AML cell experiments shown in Figure S13D, cells were plated in duplicate at 2×10^5 cells/mL into round-bottom 96 wells. Viability was assessed by PI or DAPI (0.5 μg/mL). Live cells were quantified using a Cytoflex flow cytometer (Beckman Coulter). Data analysis was performed using FlowJo v10 (BD Biosciences) and Prism v9.

Please cite this article in press as: Diepstraten et al., Putting the STING back into BH3-mimetic drugs for *TP53*-mutant blood cancers, Cancer Cell (2024), https://doi.org/10.1016/j.ccell.2024.04.004

Primary specimen death assays

Cells were plated at 1.5–5 × 10^5 cells/mL into 96 well round-bottom plates and cultured at the indicated drug concentrations for 48 h at 37°C and 5% CO_2. Cell viability was assessed by flow cytometry using the NovoCyte Quanteon (Agilent) or Cytek Aurora (Cytek Biosciences). For AML samples, leukemia cells were identified by staining for CD117. Cells were stained with extracellular markers to enable lineage identification. Antibodies used for these assays are listed in the key resources table. Viability was assessed by staining with PI (0.5 μg/mL) or DAPI (0.2 μg/mL). Data analysis was performed using FlowJo v10.

Immunoblotting

Immunoblotting was performed as described previously.[20] Briefly, cells were treated with S63845, venetoclax, A-1331852, STING agonists or Nutlin-3a (MedChemExpress #HY-10029) after being pre-treated with 25 μM of the broad-spectrum caspase inhibitor QVD-*O*-Ph (MedChemExpress #HY-12305) for 15 min. Protein concentration was measured using the Pierce BCA Protein Assay Kit (Thermo Fisher Scientific #23225). 10 μg of protein was loaded per sample. For AML cells, immunoblotting was performed as described previously.[61] Extracts from equal cell numbers were loaded per sample. Antibodies used are listed in the key resources table. Quantifications were performed using ImageJ/Fiji.[62] Levels of the proteins of interest were normalized to levels of HSP70 and data plotted in Prism v9.

Quantitative reverse transcriptase PCR

RNA extractions, cDNA syntheses and TaqMan RT-qPCRs were performed as described previously.[20] Cells were treated with S63845, venetoclax, A-1331852, STING agonists or Nutlin-3a after being pre-treated with 25 mM QVD-*O*-Ph caspase inhibitor for 15 min. Data were analyzed using the ΔΔCt method, normalized to the housekeeping control gene (*Hmbs*/*HMBS or GAPDH*) for each sample. Data were plotted in Prism v9. TaqMan probes are listed in the key resources table. In all instances, Ct values for each gene were normalized to the housekeeping gene *Hmbs*/*HMBS*, except for AML samples (which are normalized relative to *GAPDH*) while fold change is shown relative to indicated controls.

RNA-seq of *Eμ-Myc* lymphoma cells

Eμ-Myc lymphoma cells were treated with 300 nM S63845 or 100 nM diABZI after pre-treatment with QVD-*O*-Ph for 15 min. Cell pellets were collected after 24 h and resuspended in TRIzol (Thermo Fisher Scientific #15596026). RNA was extracted according to the manufacturer's instructions and 200 ng used per sample for sequencing using the TruSeq RNA Library Prep Kit v2 (Illumina #RS-122-2001), according to the manufacturer's instructions. Paired-end sequencing was performed by the WEHI genomics facility on a NextSeq 2000 (Illumina).

Generation and culture of mouse AML cells

HoxA9/*Meis1* construct[63] retrovirus was produced using GAG and ENV packaging as described previously.[64] Fetal livers from E14.5 C57BL/6-LY5.2-WEHI embryos were transduced with virus and 5 × 10^5 cells transplanted IV into sublethally irradiated (1 × 750 Rad) male C57BL/6-LY5.1-WEHI mice (6–8 weeks old), as described previously.[65] Mice were monitored for leukemia development by experienced animal technicians. *HoxA9*/*Meis1* AML cell lines (556, 557, 558, 559, 561) were generated from the bone marrow or spleen harvested from mice at ethical endpoint. Cells were maintained in Iscove's Modified Dulbecco's media (IMDM; Gibco #12440053), supplemented with 10% FBS and IL-3 (1:100, made in house).

Cell cycle and proliferation analyses

To determine cell number and viability for cell proliferation analyses, an equal volume of 0.4% trypan blue (BioRad # 1450021) was added to samples and cells were counted on a TC20 Automated Cell Counter (BioRad). Data were plotted in Prism v9. For cell cycle analyses, cells were treated with DMSO or diABZi for 24 h, then collected and fixed on ice for 30 min using the eBioscience Foxp3/Transcription Factor Staining Buffer Set (Thermo Fisher Scientific #00-5523-00). Cells were then resuspended in 1× permeabilization buffer and incubated at 4°C for at least 48 h. Cells were spun down and resuspended in PBS containing 5% FBS and 0.5 μg/mL DAPI (Sigma #D9542) and analyzed on an LSR II W flow cytometer (BD Biosciences). Data analysis was performed using FlowJo v10.

Rho^0 cells and cytosolic mtDNA analysis

To examine mtDNA release into the cytosol, DOHH2 cells were pre-treated with QVD-*O*-Ph for 15 min and then DMSO (vehicle control), S63845 (100 nM) or Thapsigargin (100 nM; Sigma Aldrich #T9033) for 4 h. Cells were collected and cytosolic DNA released into the supernatant using established protocols.[66] Briefly, cell pellets were resuspended in 1% NP-40/IGEPAL CA-630 (Sigma Aldrich #56741) and incubated on ice for 15 min. Insoluble material was pelleted by centrifugation at 13,000 rpm for 15 min at 4°C and DNA extracted from the supernatant using the DNeasy Blood & Tissue Kit (QIAGEN). Quantification of cytosolic DNA was performed by qPCR using established protocols.[66,67] Briefly, 10 ng of cytosolic DNA was amplified using SYBR Green PCR Master Mix (Thermo Fisher Scientific #4309155) and published primers[66,67] for the mtDNA gene *MT-ND1*, nuclear gene *KCNJ10*, and ribosomal DNA *18s* (listed in Table S3). Relative levels of mtDNA and nuclear DNA in the cytosol were determined by normalization to ribosomal DNA levels using the ΔΔCt method. Graphs were plotted in Prism v9.

To generate Rho^0 derivatives of the human DLBCL cell line DOHH2, cells were cultured in low doses of ethidium bromide (50 ng/μL; VWR 443922U) for 33 days, in the presence of uridine (50 μg/mL; Sigma-Aldrich #U3003) and sodium pyruvate (2 mM). Dependence

on uridine was confirmed by uridine withdrawal and quantification of cell viability and cell number 72 h later by trypan blue exclusion on a TC20 Automated Cell Counter (BioRad), as described for proliferation assays above. Whole cell DNA was extracted from pelleted cells using the DNeasy Blood & Tissue Kit (QIAGEN) and loss of mtDNA was confirmed by qPCR for the mitochondrial gene *MT-ND1* and mitochondrial DNA D loop sequence (MT-DNA-Loop) (also listed in Table S3) as described above. Levels were normalized to that of the nuclear gene *KCNJ10* using the ΔΔCt method. Graphs were plotted in Prism v9.

Imaging

Brightfield imaging of ENKT lymphoma cells was performed using a ZOE fluorescent cell imager (BioRad).

QUANTIFICATION AND STATISTICAL ANALYSIS

Statistical details for each experiment are located in their respective figure legends and, due to the large number of comparisons, additional comparisons are listed in Table S4. All data were confirmed to conform with the assumptions of the statistical tests used via normalcy tests, where appropriate. Mouse survival curves were plotted in Prism v9. Curves were compared using the Log rank (Mantel-Cox) test with Bonferroni's correction. For all other assays, comparisons between two groups were performed using an unpaired Student's t test. Comparisons between more than two groups were performed using a one-way ANOVA with Tukey's multiple comparisons test. Statistics were performed using Prism v9.

STING1 gene expression data were downloaded from the Cancer Cell Line Encyclopedia.[68] Cell lines were further annotated by Non-Hodgkin lymphoma subtype using data from Cellosaurus.[69] Boxplots were generated in R using ggplot2.[70]

For RNA-seq analysis, sequencing files were uploaded to and analyzed on the Galaxy[71] Australia (usegalaxy.org.au) server. Sequencing reads were aligned to the mouse genome (mm10) using HISAT2 v2.2.1[72] and read counts obtained for each gene using the featureCounts function of subread v2.0.3[73] (>19.4 M reads assigned to exons per sample). Differential expression analysis was performed using limma-voom v3.50.1.[74] Lowly expressed genes that did not meet a minimum expression level (count per million > 0.5) in at least 2 samples were filtered out. Normalization was performed using the trimmed mean of M-values (TMM) method.[75] The Benjamini and Hochberg method was used to adjust *p*-values for multiple tests.[76] Genes with adj. *p*-value < 0.05 and logFC > 0.58 were considered differentially expressed. Plots were generated with ggplot2 v3.3.3.[70] Gene set enrichment analysis (GSEA) was performed using the Molecular Signatures Database Hallmark Gene Set Collection[77,78] (mapped to mouse orthologues[79]) with fgsea v1.8.0.[80] Gene sets with adj. *p*-value $\leq$ 0.0015 were plotted in Prism v9.